White Rose Research Online

eprints@whiterose.ac.uk
https://eprints.whiterose.ac.uk
Universities of Leeds, Sheffield and York

Deposited via The University of Sheffield.

White Rose Research Online URL for this paper:
https://eprints.whiterose.ac.uk/id/eprint/246783/

Version: Published Version

Article:
Godson, B., Lyman, J., Pursiainen, M. et al. (2026) The Gravitational-wave Optical Transient Observer (GOTO) Fast Analysis and Spectroscopy of Transients (FAST) surveys. Monthly Notices of the Royal Astronomical Society, 552 (3). stag1848. ISSN: 0035-8711

https://doi.org/10.1093/mnras/stag1848

Reuse
This article is distributed under the terms of the Creative Commons Attribution (CC BY) licence. This licence allows you to distribute, remix, tweak, and build upon the work, even commercially, as long as you credit the authors for the original work. More information and the full terms of the licence here: https://creativecommons.org/licenses/

Takedown
If you consider content in White Rose Research Online to be in breach of UK law, please notify us by emailing eprints@whiterose.ac.uk including the URL of the record and the reason for the withdrawal request.

UNIVERSITY OF LEEDS
University of Sheffield
UNIVERSITY of York

Monthly Notices of the ROYAL ASTRONOMICAL SOCIETY

MNRAS **552,** 1–19 (2026)
https://doi.org/10.1093/mnras/stag1848
Advance Access publication 2026 September 26

The Gravitational-wave Optical Transient Observer (GOTO) Fast Analysis and Spectroscopy of Transients (FAST) Surveys

B. Godson [1★] J. Lyman [1] M. Pursiainen [1] D. Steeghs [1] B. D. R. Davies [1,2] M. J. Dyer [3,4] N. Koivisto,[5] M. A. Mitchell [1] D. O'Neill,[6] B. Warwick [1] S. Belkin [7] P. Chote [1] D. L. Coppejans,[1] R. Eyles-Ferris [8] D. Jarvis,[3] Y. Julakanti,[8] L. Kelsey [9] M. Kennedy [10] T. Killestein [1] A. Kumar,[11] A. Levan,[12] S. Littlefair,[3] M. Magee,[1] S. Mandhai,[13] D. Mata Sánchez [14,15] S. Mattila,[5,16] J. McCormac,[1] J. Mills,[1] S. Moran,[8] J. Mullaney,[3] C. Phillips,[1] D. Pollacco,[1] K. Pu,[7] A. Sahu,[1] U. Sawangwit,[17] M. Shrestha,[7] E. Stanway [1] R. Starling,[8] Y. Sun [8] K. Ulaczyk,[1] L. Vincetti,[18] E. Wickens,[19] K. Wiersema,[20] D. K. Galloway,[7,21] V. S. Dhillon [3,14] P. O'Brien,[8] G. Ramsay [18] K. Noysena,[17] R. Kotak,[5] R. P. Breton [13] L. K. Nuttall,[19] B. Gompertz [6] and J. Casares [14]

Affiliations are listed at the end of the paper

Accepted 2026 September 25. Received 2026 September 23; in original form 2026 July 6

ABSTRACT

The study of young and fast astronomical transients is often limited by the difficulty of acquiring data, particularly spectra, within hours to days of explosion. Historically, follow-up programmes have rarely obtained spectra until many days after discovery; coupled with lower-cadence discovery observations, this has meant that the early evolution of transients has not been systematically probed. The Fast Analysis and Spectroscopy of Transients (FAST) programme aims to build a rich data set on the early evolution of a range of transients by linking a high-cadence discovery survey on the Gravitational-wave Optical Transient Observer (GOTO) with immediate visitor-mode spectroscopic follow-up. We report results from two prototype runs, FAST 23 and 24, carried out in August 2023 and February 2024 using the 2.54 m Isaac Newton Telescope. Between these, 51 transient classifications were reported, 19 of which were discovered by GOTO with a median time between discovery and first spectrum of < 2 d. We highlight the discovery and characterization of SN 2024cld, enabled by spectroscopic observations beginning within 30 min of discovery, which reveals the complex mass-loss history of an evolved supergiant star in its final years prior to supernova. Further GOTO–FAST runs are ongoing at the Nordic Optical Telescope, and we hope this paper will be informative for those considering the creation of similar programmes.

Key words: methods: observational – supernovae: general – transients: supernovae.

1 INTRODUCTION

Explosive transients provide a unique opportunity to study physics in the universe at its most extreme. They reveal the final stages of stellar and binary evolution and have played a crucial role in time-domain astronomy since the early photographic plate surveys. Technological advances in large format digital detectors and computing have been exploited over the last decade by surveys such as the Panoramic Survey Telescope and Rapid Response System (Pan-STARRS; K. C. Chambers et al. 2016), the Zwicky Transient Facility (ZTF; E. C. Bellm et al. 2018), the Asteroid Terrestrial-impact Last Alert System (ATLAS; J. L. Tonry et al. 2018a), the Large Array Survey Telescope (E. O. Ofek et al. 2023), the Wide Field Survey Telescope (T. Wang et al. 2023), and BlackGEM (P. J. Groot et al. 2024) to dramatically increase the rate at which new transients are discovered. Over the next decade the field will experience another step-change in the rate of transient discovery, with the start of the Legacy Survey of Space and Time carried out by the NSF–DOE Vera C. Rubin Observatory ({. Ivezić et al. 2019) and the development of all-sky monitoring systems such as the Digital Telescope (see S. Bowler 2025 for an overview) and the Argus Array (N. Law et al. 2022; N. M. Law et al. 2022).

Despite the improved cadence and depth of modern wide-field transient surveys, the diverse behaviour of optical transients in the hours and days immediately following their explosion remains poorly explored by observations. Their discovery in early wide-field surveys traditionally occurred near or after they reach peak brightness, and observations of earlier times are mostly a result of serendipitous coverage rather than a systematic exploration. In the last decade, a number of surveys have been

★ E-mail: benjamin.godson@warwick.ac.uk

© The Author(s) 2026.
Published by Oxford University Press on behalf of Royal Astronomical Society. This is an Open Access article distributed under the terms of the Creative Commons Attribution License (https://creativecommons.org/licenses/by/4.0/), which permits unrestricted reuse, distribution, and reproduction in any medium, provided the original work is properly cited.

Downloaded from academic.oup.com/mnras/article/552/3/stag1848/8836714 by guest on 21 October 2026

undertaken which target these early time-scales by observing at higher cadence over reduced areas of the sky. Dedicated transient surveys include the High cadence Transient Survey (HiTS; F. Förster et al. 2016), which targeted a 2 h cadence, over 120–150 deg^2 of sky, to a depth of $r = 23$–24 and the Young Supernova Experiment (YSE; D. O. Jones et al. 2021), which utilizes Pan-STARRS to observe 1500 deg^2 at a 3 d cadence. Sub-surveys targeting high cadences have also been undertaken by ZTF, such as the high-cadence experiment (T. Ahumada et al. 2023), which aimed for intra-night observations over 4680 deg^2 of sky for three nights in 2023, with the goal of improving detection efficiency for fast-evolving and young transients. The currently running ZTF + LSST Inventory of Nuclear Transients and Supernovae (Z + LIONS; K. Hinds et al. 2026) programme combines a spectroscopic follow-up programme with a one day cadence ZTF survey of the overlap region between ZTF and the LSST Wide-Fast-Deep footprint. Modern exoplanet surveys, such as the Transiting Exoplanet Survey Satellite (*TESS*; G. R. Ricker et al. 2015), also operate at very high cadences, providing near continuous monitoring over large parts of the sky, and have serendipitously provided dense photometric coverage of transients at early times (e.g. M. M. Fausnaugh et al. 2021, 2023).

Supernovae (SNe) are the most commonly observed extragalactic transients, making up the majority of the >20 000 transients discovered each year. Although SNe remain active on time-scales of months to years, their early-time evolution can encode unique information about their progenitor systems and explosion mechanisms. After the core collapse of a massive star, the photoionization of circumstellar material (CSM) by ultraviolet and X-ray photons, released when the supernova shock breaks out of the surface of the star, enables the use of flash spectroscopy (e.g. A. Gal-Yam et al. 2014; D. Khazov et al. 2016; C. S. Kochanek 2019; K. A. Bostroem et al. 2023). As the shock-breakout flash expands, the evolution of these spectral features can be used to probe the density profile and composition of the CSM it passes through, which can be used to constrain the mass-loss history of the SN progenitor. These features are typically present for only a few days post-explosion and observations at earlier epochs probe the CSM closer to the progenitor. The study of these features, and other early-time interaction signatures, has motivated the development of spectroscopic follow-up programmes which specifically target infant transients (e.g. R. J. Bruch et al. 2023).

Photometric surveys have also revealed multiple populations of extragalactic transients that evolve on much faster time-scales (M. R. Drout et al. 2014; M. Pursiainen et al. 2018), many of which cannot be adequately explained by standard supernova models powered by radioactive decay (S. J. Prentice et al. 2018; Z. Cao et al. 2024). Fast blue optical transients (FBOTs) and their luminous subclass (LFBOTs) are of particular astrophysical interest, and despite the discovery of numerous candidates, since the well-observed AT 2018cow (S. J. Prentice et al. 2018), there is no consensus on their origin or mechanism and significant diversity within known examples (e.g. C. P. Gutiérrez et al. 2024). Although the high grasp of current surveys (E. O. Ofek & S. Ben-Ami 2020; E. O. Ofek et al. 2023) has increased the rate at which fast transients are discovered, effective follow-up of these objects remains challenging. The fast evolution of their optical light curves, with rise times $\lesssim 5$ d, are poorly sampled by most all-sky surveys, typically requiring dedicated observing campaigns triggered at early times to obtain more than a few measurements. The rate of LFBOTs is very low, less than 0.6 per cent of the local core-collapse supernova rate (A. Y. Q. Ho et al. 2023), which means that well observed examples are few and far between. Combined with their ambiguous nature they remain of high-interest to rapidly identify and follow-up.

Increasing discovery rates have also revealed many other classes of intrinsically rare transients, which make up only a few per cent or less of the total population and span a wide range of energy scales and environments. Many classes of underluminous transients have been identified with luminosities between that of classical novae and typical supernovae. Some of these, such as calcium-rich SNe (e.g. W. V. Jacobson-Galán et al. 2022; C. G. Touchard-Paxton et al. 2025) and type Iax SNe (R. J. Foley et al. 2013), are considered subclasses of supernovae. There are also two families of gap transient characterized by red colour and very low expansion velocities ($\lesssim 1000$ km s^{-1}), these are the luminous red novae (LRNe) and intermediate luminosity red transients (ILRTs). LRNe are typically associated with the final stages of common-envelope evolution, with a massive ejection, possibly followed by stellar merger (A. Pastorello et al. 2019). The origins of ILRTs are slightly less clear, they are typically attributed to electron-capture SNe (e.g. T. A. Thompson et al. 2009; S. Rose et al. 2025; G. Valerin et al. 2025) but other proposed models include explosions of blue supergiants (T. J. Moriya & A. Menon 2024), non-terminal outbursts in dusty luminous blue variables (J. E. Andrews et al. 2021), and failed supernovae (D. Tsuna et al. 2020). At higher energies, tidal disruption events (TDEs) and extreme nuclear transients (ENTs; e.g. J. T. Hinkle et al. 2025) are highly luminous events occurring within the nuclei of galaxies, powered by the disruption of stars passing within the tidal disruption radius of massive black holes (M. J. Rees 1988). The characteristics and rates of these events are important probes of the properties (e.g. S. Velzen et al. 2020) and populations (e.g. N. C. Stone & B. D. Metzger 2016) of dormant massive black holes, which are otherwise difficult to study.

It is clear that there are still significant gaps in our understanding as we continue to push the parameter space of known transients to faster time-scales, both in terms of novel intrinsically fast transients and the early time behaviour of more well-known classes. While discovery rates continue to increase, our ability to carry out spectroscopic follow-up is still limited. Only a small fraction of transients (≈ 10 per cent) are classified spectroscopically, typically based on observations made several days or weeks after discovery, at which point much of the pre-peak photometric and spectroscopic evolution of the transient may have been missed. This is discussed in more detail in Section 3.4. Classification efforts are typically carried out by large observing programmes at 2–4 m class telescopes, such as the advanced Public ESO Spectroscopic Survey of Transient Objects (ePESSTO+; S. J. Smartt et al. 2015) and its successors on the New Technology Telescope. Combining discovery surveys with dedicated spectroscopic follow-up, as in the ZTF Bright Transient Survey (BTS; C. Fremling et al. 2020) has also proven very effective at delivering spectroscopically complete transient samples (e.g D. A. Perley et al. 2020). Early-time spectroscopy can provide unique information about the progenitors, environments and mechanisms. Rapid classification of transients also enables prioritization of follow-up resources to study their early evolution, which is often very diverse even for transients with similar late-time behaviour.

The Gravitational-wave Optical Transient Observer (GOTO; D. Steeghs et al. 2022; M. J. Dyer et al. 2024) is an array of wide-field optical telescopes optimized for the discovery of electromagnetic counterparts to gravitational wave (GW) events.

Downloaded from academic.oup.com/mnras/article/552/3/stag1848/8836714 by guest on 21 October 2026

Comprising four systems at two near-antipodal sites, GOTO is capable of surveying the entire night sky with a cadence of 2–3 d (M. J. Dyer et al. 2020). Currently, GOTO responds automatically to the detection of gravitational waves by the LIGO–Virgo–KAGRA (LVK) collaboration (B. P. Abbott et al. 2020), triggering automatic follow-up campaigns in response to events likely to result in optical emission (B. Gompertz et al. 2020, Ackley and Dyer et al., In preparation). Additionally, GOTO responds to detections of gamma-ray bursts (GRBs) by the *Fermi* Gamma-Ray Burst Monitor (GBM; D. J. Thompson & C. A. Wilson-Hodge 2023), the *Swift* Burst Alert Telescope (BAT; L. Angelini et al. 2022), and the *SVOM* Gamma-Ray Monitor (YU. Shun-jing et al. 2020) to search for optical afterglows (e.g. A. Kumar et al. 2025; S. Belkin et al. 2026), as well as real-time neutrino detection alerts from the IceCube neutrino observatory (M. G. Aartsen et al. 2017; E. Blaufuss et al. 2019). The northern site (GOTO-N) is located at the Roque de los Muchachos Observatory (ORM) on the island of La Palma, Spain, while the southern site (GOTO-S) is located at the Siding Spring Observatory (SSO) in New South Wales, Australia. More than 13 000 astronomical transients have been reported by GOTO since the completion of GOTO-S in May 2023, with over 5000 of those being first discovered by GOTO.

Alongside GOTO-N, the ORM hosts a large number of telescopes and instruments spanning a wide range of apertures, observing modes and capabilities, many of which are well suited to the study of astronomical transients. The Isaac Newton Telescope (INT), with its Intermediate Dispersion Spectrograph (IDS), is one such facility, a 2.54 m optical telescope capable of spectroscopic observations of the majority of targets discovered by GOTO.

The Fast Analysis and Spectroscopy of Transients (GOTO–FAST) programme combines GOTO's highly automated transient discovery capabilities with the INT and other complementary facilities, both at the ORM and elsewhere, to provide low-latency spectroscopic observations and classifications of transients. GOTO–FAST observing runs couple a high-cadence discovery survey to immediate spectroscopic follow-up, in order to minimize the time between the appearance of a transient and its first spectrum. We describe the first two observing runs, hereafter referred to as FAST 23 and FAST 24, which were carried out during the 2023B and 2024A observing semesters of the INT. Each combined ten nights of visitor-mode observations using INT/IDS with a dedicated, high-cadence, GOTO discovery survey.

In Section 2 we detail the discovery survey, spectroscopic observations, and transient classification methods employed by GOTO–FAST. We then, in Section 3, review the ability of the programme to achieve its main goals: spectroscopic observations of infant transients, high cadence monitoring, and timely classification of rare and/or fast transients. Finally, in Section 4, we summarize our results and discuss the current state of low latency spectroscopic follow-up of GOTO transients, and plans for future observing runs.

2 METHODS

2.1 Transient discovery with GOTO

A single GOTO system consists of eight unit telescopes (UTs) with offset, but slightly overlapping, fields of view. These UTs are equipped with identical cameras, focusers, and filter wheels to operate together as a single telescope with an approximately 44 deg^2 field of view. To enable rapid follow-up of external alerts, GOTO is capable of autonomous observing, without human intervention, through the GOTO-Telescope Control System (G-TeCS), described in full by M. J. Dyer (2020). Observations across the whole sky are made on a fixed grid of 1048 tiles; each with an area corresponding to the field of view of a single GOTO system. In the absence of external triggers, GOTO typically performs an all-sky survey, covering the visible sky with a cadence of 2–3 d and, depending on sky brightness, a limiting AB magnitude of 19–21 mag in the GOTO-*L* band (M. J. Dyer et al. 2020). The all-sky survey is a useful tool for studying a wide variety of time-varying sources, including novae (T. L. Killestein et al. 2025b; S. Khamrat et al. 2026), symbiotic binaries (G. Ramsay et al. 2026), and Solar-system objects (N. Kongsathitporn et al. 2024; A. F. Gillan et al. 2026). During follow-up of alerts, these observations give constraints on the time of appearance of new sources and also allow for serendipitous discovery of transients.

A standard all-sky survey observation consists of four images in the GOTO-*L* band, each with an exposure time of 45 s, which are co-added into a set image with a total exposure time of 180 s. Taking into account overheads for mount pointing, focus of the telescopes, and camera readout, a typical observation takes 280 ± 10 s. Both the exposure time and number of exposures can be increased in situations where increased depth is desired in exchange for a decrease in survey speed, such as follow-up observations of GRBs with well-constrained localizations. The *L* band is based on a broad-band luminance filter which transmits light between 400–700 nm. While each GOTO system is equipped with additional filters to allow for RGB colour imaging, they are currently not used for routine survey or follow-up observations. An autonomous scheduler selects possible observations from a central data base shared between all GOTO systems based on their priority (rank), observational constraints, and a heuristic tiebreaker primarily based on airmass.

To detect new sources in the sky within an image, it is necessary to have a reference with which to compare. Each GOTO tile has an associated reference image (template) covering the same area of sky, created from a set of observations with a much longer total exposure time (720 s) to reach a fainter limiting magnitude than that of normal survey images. These templates are used to perform difference imaging, and each was manually inspected to ensure sufficient depth, resolution, and a lack of artefacts which would generate bogus detections.

Raw images are transferred to the University of Warwick for processing by GOTO's KADMILOS data processing pipeline (J. D. Lyman et al. 2026). This performs standard CCD calibration tasks, as well as image alignment and stacking, astrometry, photometry, and difference imaging using HOTPANTS (A. Becker 2015). After template subtraction, any transient or varying sources are extracted from the difference images for further classification. In addition to real astrophysical sources within the difference images, there is significant contamination from artefacts that make manual vetting of every detection infeasible. A real-bogus classifier based on a Bayesian convolutional neural network (T. L. Killestein et al. 2021) is used to filter the majority of false positive detections. Candidates with a high real-bogus score pass into the GOTO Marshall, a web-based application used to perform human vetting and reporting of transients.

Typically, the time from shutter close on the final image in a visit to transient candidates appearing in the Marshall is on the order of 10 min. This is an important metric for GOTO, as being able to rapidly review candidates is essential during

Downloaded from academic.oup.com/mnras/article/552/3/stag1848/8836714 by guest on 21 October 2026

a multi-messenger follow-up campaign. Optimizations made to the pipeline and Marshall for this purpose also benefit prompt discovery and rapid follow-up of fast transients.

Within the Marshall, photometry of detected sources is provided alongside cutouts of the discovery, template and difference images, and contextual information such as the likely host galaxy (if any), Galactic latitude, and extinction. Candidates' positions are compared to known Solar system objects, and any matches to exact or nearby coordinates are shown to users in the Marshall. Using this information, sources are vetted by astronomers into different categories. Any remaining image artefacts that were not identified by the real-bogus classifier are discarded, as are real detections of moving objects (e.g. minor planets, comets, and artificial satellites). Of the remaining astrophysically real sources, only a small subset is of interest for extragalactic transient discovery; the rest are primarily variable sources such as variable stars and active galactic nuclei (AGNs) or Galactic transients (cataclysmic variable outbursts, dwarf novae, etc.) which are identified and stored for later analysis. The final vetting option is the GOTO transient stream, sources vetted to the stream (streamed objects) are very likely to be real extragalactic transients and are reported to the Transient Name Server (TNS)[1] soon after being vetted.

In addition to those sent to the Marshall, another set of sources with a uniform real-bogus distribution is selected to be sent to *Kilonova Seekers*[2] (Killestein and Kelsey et al. 2024), a citizen science project built to rapidly identify transients within the GOTO data stream. In *Kilonova Seekers*, volunteers are shown image cutouts and asked if they believe the marked detection to be a real astrophysical source. When a consensus is reached, candidates considered to be bogus are retired and will not be shown to more volunteers, while those considered to be real are sent to the Marshall and an alert is sent to the GOTO team.

All GOTO photometry is calibrated against ATLAS Refcat2 (J. L. Tonry et al. 2018b) and reported as AB magnitudes in the GOTO-L band (L). For further details see J. D. Lyman et al. (2026). Non-detections are given as 5σ limiting magnitudes unless otherwise specified.

2.1.1 *High cadence survey*

Cadence refers to the frequency or period at which observations are taken of a given area of the sky. A high (or short) cadence refers to a shorter period of time between consecutive observations, whereas a low (or long) cadence refers to a longer period of time. The GOTO all-sky survey provides a typical cadence of 2–3 d, optimized to provide informative non-detections during targeted gravitational-wave follow-up campaigns. This cadence is very well suited to GOTO's primary science goals as well as a number of complementary objectives such as the study of variable stars and the discovery of classical extragalactic transients.

With the cadence of the all-sky survey, events can be up to 3 d old at the time of discovery. Without higher cadence observations, it is difficult to determine the exact age which makes targeting infant transients difficult. Taking observations at a higher cadence decreases the average time between a transient becoming active and being discovered as well as allowing us to better constrain its age.

As the time taken by GOTO to survey a given area of the sky is approximately constant, the simplest way to achieve a higher cadence is by restricting observations to a smaller area of the sky. Although this decreases the overall volume of space being surveyed and, therefore, the rate at which transients are discovered, those which are discovered will, on average, be found at earlier phases. The existing scheduler system can achieve this by creating a survey with a limited set of tiles which are valid for re-observation on a short time-scale. A higher cadence could also be achieved by reducing the exposure time of each GOTO observation; however, this decreases sensitivity and makes each observation less efficient because of fixed-duration overheads (see Fig. 2).

During planning of the FAST 23, only around 25 per cent of the sky was covered by tiles with valid templates. Observations outside of this region could not be processed using difference imaging and so those areas were excluded from the high-cadence survey. Additionally, at this time only GOTO-N was available as GOTO-S was still undergoing commissioning. The tile selections for each survey were determined based on the following priorities:

(i) Each tile must have an associated completed template to allow for difference imaging.
(ii) Tiles with high Galactic extinction should be excluded, because of the reduced probability of extragalactic transient detection.
(iii) Tiles should be chosen across a range of right ascension (RA) to ensure visibility throughout the night, with a preference for tiles which are rising at the start of night.
(iv) The total number of tiles should be limited such that tiles can be observed multiple times each night.

The final tile selections for both surveys are shown in Fig. 1. During FAST 23, the survey consisted of 75 tiles, covering an area of 3470 square degrees. The exact tile selections here were almost completely constrained by the requirement for valid templates and avoiding the Galactic plane. In the lead up to FAST 23, there was a deliberate effort to produce and verify a large number of template images in order to increase available area. As each GOTO tile is in-fact made up of 8 individual fields, one for each of the UTs within a single GOTO system, manually verifying each template was a considerable task. In the final month before the survey start, the number of tiles with a complete set of templates rose from 95 to 257, of which 150 were visible for at least part of the night. Excluding tiles near the Galactic plane and the extremes of the right ascension range resulted in the final selection.

By FAST 24, the second GOTO site in the southern hemisphere (GOTO-S) was operational at Siding Spring Observatory (SSO); with visibility of declinations between -90° and $+30^\circ$. SSO is approximately antipodal to GOTO-N, giving almost constant coverage of the area of sky ($-30^\circ \lesssim$ Dec. $\lesssim +30^\circ$) observable by both nodes. To take advantage of this, an equatorial band of the sky with declinations between -15° and 30°, observable by GOTO-N/S and the INT, was chosen as the basis for the FAST 24 survey. Template images are not shared between the two GOTO sites, so the valid tiles are not the same between them, although there is significant overlap. Effectively, this meant that the survey consisted of three sets of tiles; two sets observed only by GOTO-N or GOTO-S, respectively, and one observed by both. Priority was given to tiles for which both sites had templates and additional tiles were added to the survey for both hemispheres based on the same criteria as in FAST 23.

[1] http://www.wis-tns.org
[2] http://kilonova-seekers.org/

Downloaded from academic.oup.com/mnras/article/552/3/stag1848/8836714 by guest on 21 October 2026

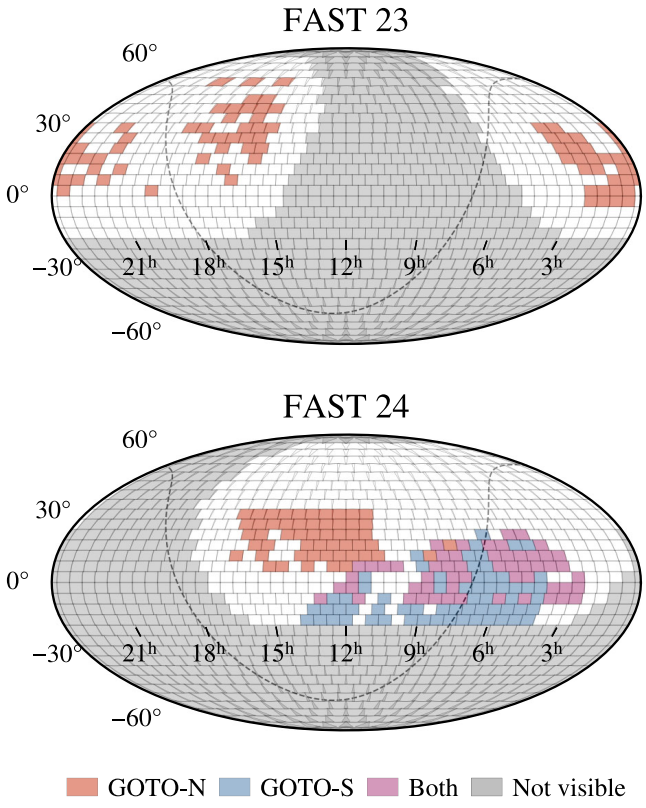


Figure 1. GOTO tiles selected for the FAST 23 (top) and FAST 24 (bottom) surveys shown on a Mollweide projection of the sky. The dashed line shows the position of the Galactic plane. Red tiles were observed by GOTO-N, blue tiles by GOTO-S and purple tiles by both. Tiles shaded in grey were not observable from La Palma during the survey dates.

During FAST 24, we chose to use only three GOTO systems for the high cadence survey, both systems in GOTO-S and one at GOTO-N. This decision was made as template coverage in the northern hemisphere had fallen behind the southern hemisphere, at the right ascensions visible at the time, due to observations taken the previous year failing quality control. As the FAST observing runs coincided with valuable dark time, GOTO-1 was left to carry out a template survey to attempt to resolve this disparity. However, during the course of the survey, one camera on GOTO-2 failed and was replaced. The replacement was fully functional, but did not have a large set of calibration files, and so while the data was still useful it could not be immediately reduced. At this point we allocated GOTO-2 to the template survey, as there was no need for timely reductions, and GOTO-1 to the FAST survey. For the majority of FAST 24, GOTO 1, 3, and 4 were carrying out the discovery survey.

In total, 171 tiles were included, with a combined area of 7381 square degrees. Of these tiles, 108 were valid for observation by GOTO-N and 118 were valid for GOTO-S. A summary of the FAST and all-sky surveys is shown in Table 1.

For both surveys, the tile lists were inserted into the observation database with a higher priority than the all-sky and template surveys but lower than externally triggered GW/GRB/Neutrino follow-up programmes. This ensured that the scheduler would prioritize FAST tiles whilst remaining responsive in the event of a GRB or GW event, and would fall back to the regular sky surveys if no FAST observations were valid. FAST 23 took place during the LVK O4 observing run, and estimates of the binary neutron star (BNS) merger rate prior to the start of O4 (A. Colombo et al. 2022) implied a reasonable probability of overlap between GOTO–FAST and a BNS merger follow-up campaign. FAST 24 was scheduled within the gap between LVK O4a and b, which allowed more flexibility, since maintaining cadence on fields outside the survey region was less important.

Table 1. Survey details for GOTO–FAST and the GOTO all-sky surveys. Image sets refers to the number of exposures which are co-added and their exposure time in seconds. Targets from the template survey are observed only once, assuming that observation is of sufficient quality, and so the cadence is not defined.

Survey	Image sets	Telescopes	N_{Tiles}	Area (deg^2)	Cadence (h)
All-Sky	4x45 s	All	1048	41,253	48–72
Template	12x60 s	All	1048	41,253	N/A
FAST 23	3x60 s	1, 2	74	3470	4
FAST 24	3x45 s	1/2*, 3, 4	171	7381	4

Note. *Mid-run change from GOTO 1 to GOTO 2 due to camera replacement.

Table 2. INT programme and time allocations for each FAST run. Time allocations are split into bright (B), grey (G), and dark (D) time corresponding to different lunar phases.

Survey	INT Programme	Allocated nights	Dates
FAST 23	I/2023B/08	3D 7G	2023 Aug 9–18
FAST 24	I/2024A/07	3D 7G	2024 Feb 4–13

The observational constraints given to the scheduler were identical to those of the all-sky survey, which limits observations to those tiles which have an altitude and moon separation greater than 30 deg, but with the minimum wait time between repeat observations reduced to 4 h, allowing multiple observations of each tile per night.

2.2 Spectroscopy with The Isaac Newton Telescope

Each GOTO–FAST survey was scheduled to run alongside a 10-night visitor-mode observing programme at the INT with the IDS instrument; spanning the nights between 2023 August 9–18 and 2024 February 4–13, respectively. The details of these time allocations are shown in Table 2. IDS is a versatile long slit spectrograph that was mounted at the Cassegrain focus of the INT and available as a common-user instrument until June 2024, when refurbishment began on the INT to prepare it for use with HARPS3 (S. J. Thompson et al. 2016).

The co-location of the INT and GOTO-N at the ORM offers a number of advantages, the most obvious of which is that tiles observed by GOTO-N are immediately observable by the INT. Additionally, in the unlikely event of hardware issues with GOTO which require physical intervention, the visiting astronomers are nearby and able to carry out this work. A follow-up programme conducted at another observatory also carries the risk that poor conditions at the ORM could result in a lack of targets, even if conditions are excellent at the follow-up site.

The primary goal of our initial spectroscopic observations was the rapid identification and classification of intrinsically rare or young transients. Targets were prioritized by human vetters on the basis of age, photometric evolution, and contextual information such as co-localization with a nearby galaxy. The highest priority was given to recently discovered targets with tight

Downloaded from academic.oup.com/mnras/article/552/3/stag1848/8836714 by guest on 21 October 2026

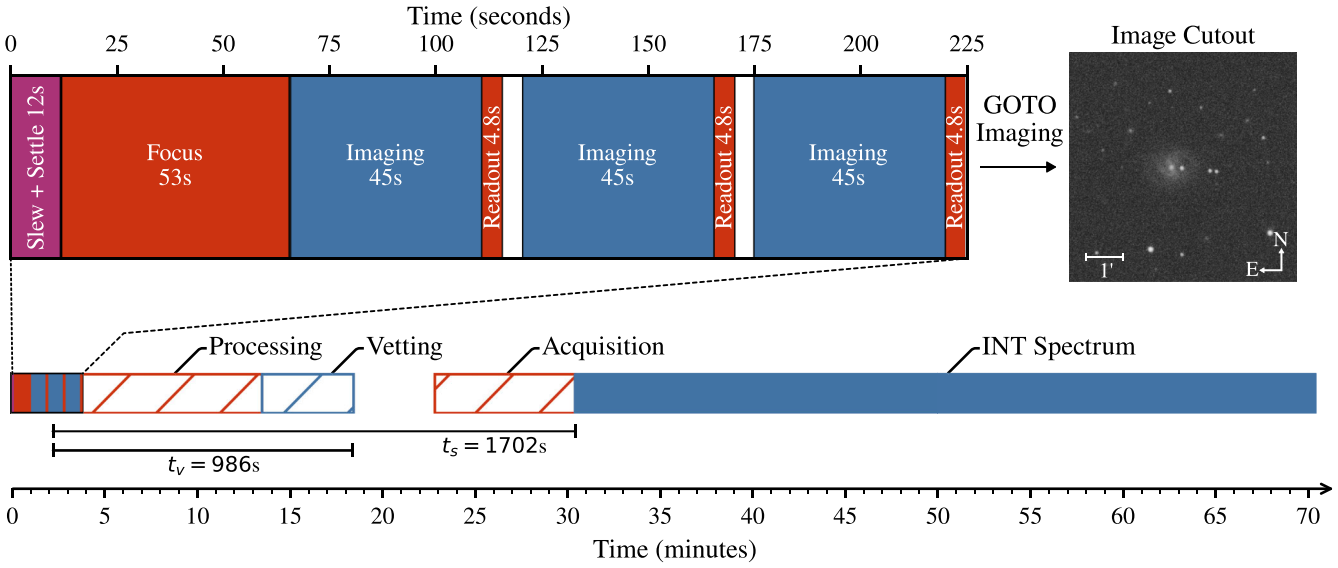


Figure 2. Timeline of the discovery and first spectrum of 2024cld from the discovery observation being selected by the telescope control system until the end of the first spectrum. The time-to-vetting t_v and time-to-spectrum t_s are defined as the time between the mid-point of the GOTO discovery observation and the end of vetting and the start of the INT observation respectively. The vetting phase is defined from when the initial detection was ingested in the GOTO Marshall until it was identified as a likely-real transient and sent to the stream. Acquisition refers to the time between the end of the previous IDS spectrum and the start of the observation for 2024cld, this primarily involved target acquisition using a blind offset and guide star acquisition.

constraints on their time of appearance and fast photometric evolution. Fig. 2 shows the breakdown of time between discovery imaging and the first spectrum for one GOTO–FAST target.

While most of these high-priority targets were expected to come from the GOTO–FAST high-cadence survey, a number of other transients were selected from the TNS using the same criteria. This was to ensure the INT could be utilized even when no targets provided by GOTO were available. The majority of these secondary targets were discovered by ZTF and ATLAS, with two more discovered by the Xingming Sky Survey Project (XOSS)[3] and one by the All Sky Automated Survey for SuperNovae (ASAS–SN; B. J. Shappee et al. 2014). In addition to classifications, our observing schedule allowed time for regular spectroscopic monitoring of up to two bright sources ($L < 18$ mag) identified during the course of the observing run.

2.2.1 Observations

All targets were observed using the RED+2 detector with the R150V grating, a GG395 order-sorting filter, and a slit width of 1 arcsec. This results in a dispersion of 0.4 nm pixel^{-1}, a spectral resolution of $R \simeq 600$, and spectra that are free from contamination by 2nd order diffraction from 395–700 nm. This low dispersion grating was chosen as it allows for observations of fainter transients, and spectroscopic classifications of transients are typically based on the presence of broad features that do not require high spectral resolution to be identified. The configuration used was the same for both FAST observing runs, with the exception of the CCD binning being changed from 1 × 1 during FAST 23 to 2 × 1 in FAST 24, providing a modest increase to the signal-to-noise ratio (S/N) at the expense of spatial sampling. The SIGNAL calculator (C. Benn 2014) was used to determine exposure times, aiming to achieve a S/N of ≥ 50 for bright ($L \leq 18$ mag) sources and ≥ 10 for the faintest transients detectable by GOTO ($L \simeq 20.5$ mag) with a nominal maximum exposure time of 1 h. For faint targets, the exposure time was divided between multiple consecutive exposures which were later co-added to mitigate the effect of cosmic-ray strikes, with a small increase in the total exposure time to account for the additional read-noise introduced.

It was expected that the majority of targets would be too faint to appear in short exposure time images with the IDS acquisition camera, so nearby bright stars were selected and on-sky offsets calculated to allow for target acquisition via blind offsetting. Positioning of these targets within the slit was confirmed with long exposure time imaging with the acquisition camera during spectroscopic observations. During parts of FAST 23, the telescope autoguiding system was unable to acquire a guide star. For these targets, tracking corrections were applied by hand while monitoring the image of the target in the acquisition camera. IDS is mounted on a rotating turntable that allows observers to set the position angle of the slit. For the majority of our observations, the spectrograph slit was aligned with the parallactic angle at the mid-point of each observation to reduce losses due to atmospheric dispersion. The details of the observations for each target are shown in Table A2.

2.2.2 Data reduction

Initial reductions and classifications were made immediately after data acquisition by observers to allow rapid follow-up (see Section 2.3) within the same night. These were performed using the IDSRED data reduction pipeline (T. E. Müller-Bravo 2023), modified for use with the RED+2 detector. All spectra were bias-subtracted, and flat fielding was performed using tungsten lamp flats. For observations split into multiple exposures, these were

[3] http://xjltp.china-vo.org/about-xingming.html

Downloaded from academic.oup.com/mnras/article/552/3/stag1848/8836714 by guest on 21 October 2026

co-added by taking the mean value of each set. Wavelength calibration was performed using observations of internal CuAr and CuNe arc lamps (H. Fathivavsari et al. 2013) taken at the start of each night and after each observation. Standard stars from the ING Spectrophotometric catalogue (J. Sinclair 1996) were observed at the start and end of each night and used to perform flux calibration.

These initial reductions were suitable for the classification and triage of key follow-up targets, but often resulted in imprecise wavelength and flux calibration. Later, after the end of both observing runs, spectra were reprocessed using a version of the PYPEIT PYTHON package (J. X. Prochaska et al. 2020a, b) modified with an additional recipe for use with IDS, as this gave more stable wavelength calibrations.

2.2.3 Classification & reporting

Transient spectral classifications and redshifts were determined by comparison with a bank of spectral templates using the Supernova Identification (SNID; S. Blondin & J. L. Tonry 2007) code. In many cases, a single spectrum was sufficient for classification; however, a number of sources showed few or no identifiable spectral features beyond a blue continuum. For these sources, additional spectroscopic observations were taken later in the run to determine whether any features appeared at later times. Initial redshift measurements were made based on SNID template matches, or host galaxy lines when they were present.

Initial classification was performed by the visiting astronomers during the night and, where a confident classification could be made, reported to the TNS. During the day, further reductions and classifications were performed and reported, with the results for each night summarized in a series of AstroNotes (B. Godson et al. 2023).

2.3 Further follow-up

Although discovery and classification were the primary goals of GOTO–FAST, a number of targets were expected to be worth targeting for follow-up observations by the GOTO collaboration. A small number of these (∼2–3) could be monitored using our INT spectroscopic programme, taking spectra every few nights after classification, without greatly impacting the number of transients we could classify.

In addition to GOTO-N and the INT, the ORM hosts several other facilities that are well suited to transient observations. The discovery, classification, and long-term monitoring of transients benefit from the use of telescopes over a wide range of apertures and response times. Studying the early phases of near-by transients requires wide-field robotic telescopes and high priority or disruptive target-of-opportunity (ToO) programmes on medium sized telescopes ($D \gtrapprox 2$ m) for spectroscopic observations. Following their evolution up to and over peak brightness. Spectroscopic observations of the faint nebular phase meanwhile require much larger telescopes but can be scheduled many months in advance.

The Liverpool Telescope (LT; I. A. Steele et al. 2004) is a robotic 2 m telescope adjacent to the INT that is also well suited to observations of transients, in particular its Spectrograph for the Rapid Acquisition of Transients (SPRAT; A. S. Piascik et al. 2014) instrument; a low-resolution, high-throughput, optical spectrograph.

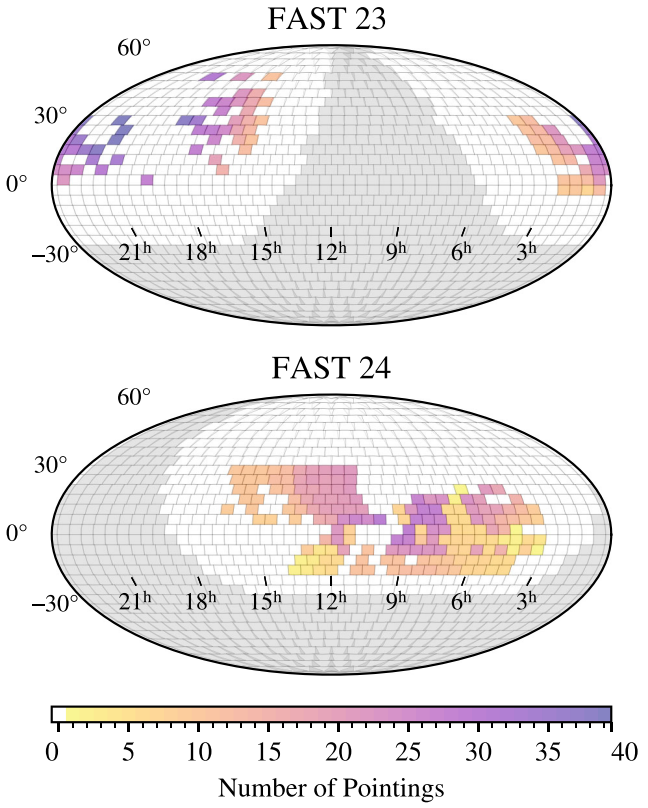


Figure 3. Mollweide projection of the sky showing the total number of observations per FAST survey tile during each observing run. Observations of other tiles (e.g. due to GRB follow-up) are excluded.

Observations using the LT can be requested using the Remote Telescope Markup Language (RTML) protocol, allowing integration with robotic telescope arrays without the need for targets to be entered by hand. This capability is integrated into the GOTO Marshall, with authorized users able to request observations of transient candidates. LT photometry and spectroscopy were obtained for a number of high-priority targets identified by GOTO–FAST, most notably SN 2024cld as detailed in Section 3.3.1.

For additional photometry, the primary facility used was pt5m (L. K. Hardy et al. 2015), a robotic 0.5 m optical telescope located on the roof of the William Herschel Telescope, approximately 200 m from GOTO-N. Observing campaigns using pt5m can also be triggered directly from the GOTO Marshall, typically being used to provide additional photometric information before a target is selected for spectroscopic follow-up, as well as for multi-band monitoring using its Johnson–Cousins *BVRI* filters. 10 targets discovered by GOTO–FAST were observed by pt5m, as well as five additional targets from other discovery sources.

3 RESULTS

3.1 High cadence survey

The total number of observations per tile and their distribution across the sky are shown in Fig. 3. Both surveys show a disparity between the tiles that are the least frequently and the most frequently observed. For FAST 23, the effect is minor and primarily caused by observational constraints, as tiles in the middle of the right ascension range are observable for a larger portion of each

Downloaded from academic.oup.com/mnras/article/552/3/stag1848/8836714 by guest on 21 October 2026

Table 3. Median time between re-observation of FAST survey tiles. Intra-night cadence includes only the time between observations taken within the same night, while median cadence considers the time between all observations.

Semester	Median intra-night cadence (h)			Median cadence (h)		
	GOTO-N	GOTO-S	Both	GOTO-N	GOTO-S	Both
FAST 23	4.12	n/a	n/a	21.5	n/a	n/a
FAST 24	4.15	4.12	4.65	22.3	47.8	14.6

Table 4. Transient sources observed by GOTO during each GOTO–FAST observing run. Candidates include all difference detections which were shown on the Marshall, excluding matches to known minor planets and *Gaia* sources. The'Stream' refers to sources identified as possible extra-galactic transients within the Marshall.

Semester	Candidates	Stream	TNS Reported	Discoveries
FAST 23	53 904	281	150	17
FAST 24	34 470	249	186	22

night. During FAST 24, however, the discrepancy is larger and primarily driven by which GOTO site each tile was observed by, though there is also a contribution from varying RA. As expected, the most frequently observed tiles were those observed by both sites, while the least frequently observed tiles were those targeted by only GOTO-S. FAST 24 took place during southern hemisphere summer, meaning nights were shorter at SSO than the ORM, and unusually poor weather at SSO further reduced the number of observations made by GOTO-S. Consequently, during FAST 24 overall, GOTO-N carried out 2753 pointings while GOTO-S carried out only 1018.

The cadence of the observations of each tile shows a distinctly bimodal distribution, with a large number of observations taking place just over 4 h after the previous observation and another large set of observations taking place approximately 22 h after the previous observation. The 4 h gap corresponds to observations of tiles taking place within a single night, just after the 4 h minimum revisit time set by the scheduler. The longer delay corresponds to observations of tiles the next night. Table 3 shows the median intra-night cadence and the overall median cadence for both surveys. During FAST 24, as explained above, the tiles observed by just GOTO-S were observed far less frequently, and so their median cadence is close to two days. Tiles observed by both sites benefited from the near continuous visibility and so, despite the smaller number of observations made by GOTO-S, had an average cadence of 14.6 h.

Another important metric for the high-cadence survey is the total number of transients detected. Table 4 shows the total number of candidates, sources sent to the Marshall stream, sources which are matched to transients reported to the TNS, and the number of those first detected by GOTO. Candidates refers to sources which passed initial automated quality control and were ingested into the Marshall, excluding matches to known minor planets. The decrease in the number of candidates between FAST 23 and 24 is attributed primarily to improvements in the pipeline and Marshall to reject spurious candidates resulting from poor registration of images. During typical operation, the vast majority of objects sent to the GOTO stream are later reported to the TNS. However, during the FAST surveys, about 1 in 4 streamed sources are not matched to TNS objects. These are primarily sources with single, poor quality, detections, which are difficult to verify. These were sent to the stream so that they could be easily monitored and targeted for follow-up if additional detections were made or no other higher priority targets were available. Under normal operations these would have remained in the pending queue until more observations were obtained.

During FAST 23, GOTO observed an average of 96 pointings per night, with a median sky coverage of 2904 square degrees. During FAST 24, the median number of tiles observed by GOTO-N per night was 138, with a median area coverage of 4286 square degrees. The median number of pointings observed by GOTO-S was 112, with a median area coverage of 3709 square degrees per night. The maximum number of pointings completed in a single night by GOTO-N was 161, which corresponds to an average of 3.88 min per three-minute observation and an observing efficiency of 77 per cent. Not included in these counts are pointings GOTO completed as part of GRB follow-up campaigns, which were given a higher scheduling priority.

3.1.1 *Effect on other GOTO surveys*

When deciding on the area and cadence of the FAST surveys, a major concern was not compromising the primary science objective of GOTO, the discovery of the optical counterparts to GW events, as well as its many complementary observing programmes. These require recent observations across the whole sky to constrain the appearance time of transients, without which it is difficult to determine if a transient was present prior to a GW or GRB detection. Additionally, at the time of both FAST surveys, template images were still being obtained across large areas of the sky which added further constraints on the amount of array time that could be used for GOTO–FAST. To quantify the effect of the FAST surveys on the all-sky survey, we calculate the cadence of GOTO observations across the entire sky during each of the FAST surveys and the fraction of observing time dedicated to them. These results do not take into account failed observations, however the impact of these is similar across all surveys given the similar exposure sets, constraints, and conditions.

Fig.4 shows the fraction of total GOTO observing time dedicated to each observation type. This includes observations taken by systems which were not involved in either FAST survey, to allow us to examine the observational'cost' of FAST relative to GOTO's other science programmes. During both surveys the largest amount of time is spent on template observations, at around 50 per cent. This may be surprising given that only one GOTO system was carrying out template observations during FAST 24. However it reflects the fact that the total amount of observations taken at GOTO-N was much higher than GOTO-S due to the aforementioned differences in weather and season. During FAST 23, GOTO-S was not involved in the FAST survey, and was dedicated almost entirely to template observations. The longer nights at SSO compared to the ORM during August,

Downloaded from academic.oup.com/mnras/article/552/3/stag1848/8836714 by guest on 21 October 2026

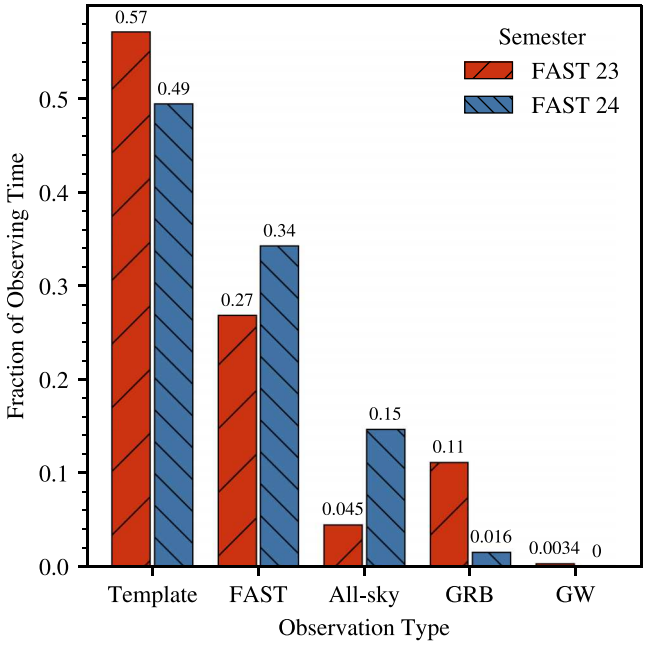


Figure 4. The fraction of GOTO exposure time used for each survey and follow-up event type during the GOTO–FAST observing runs.

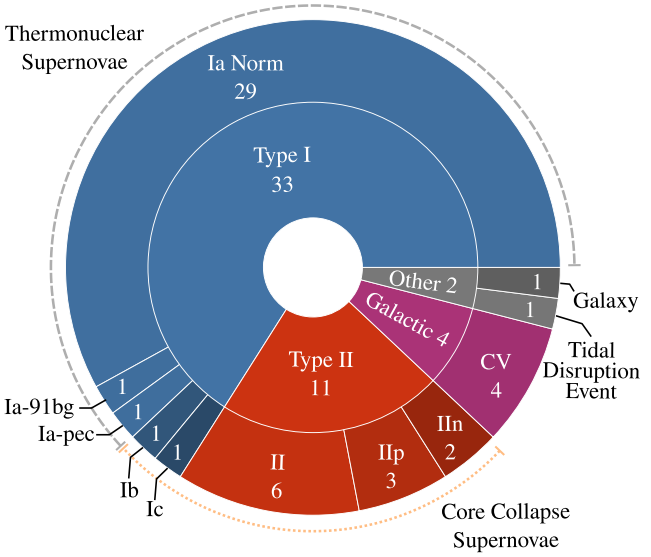


Figure 5. Classifications of transient type and sub-type (where applicable) made by GOTO–FAST. Type I supernovae are shown in shades of blue while Type II are shown in red. The outside arcs identify types associated with thermonuclear (dashed) and core collapse (dotted) supernovae. Not shown are the two sources which were classified as likely supernovae but of an indeterminate type.

combined with the lower overhead of template observations, result in the template survey making up 57 per cent of the total exposure time. A small fraction of observations were made under the all-sky survey during FAST 23, these occurred at the end of a small number of nights when there were no FAST tiles which were valid for re-observation. During FAST 24 the all-sky survey used 15 per cent of the total exposure time. These observations were taken by the GOTO system assigned to the template survey (GOTO 1 or 2) when the sky was too bright for template observations.

Observations of the FAST fields accounted for around 30 per cent of the total observing time during both surveys. This means it was relatively inexpensive in terms of GOTO observing time, and it would be feasible to run a small high cadence region without greatly impacting our all-sky cadence now that template observations are complete. This result has motivated a change in GOTO's permanent observing strategy towards a two-tiered system, with a high cadence equatorial region and lower cadence towards the celestial poles. This is described in more detail in Section 4.

GRB follow-up observations were performed during both surveys and were valid for observation with all telescopes. The large fraction of time ($\sim$ 10 per cent) used to observe GRBs during FAST 23 was primarily due to follow-up of 20 *Fermi* GBM triggers.

One gravitational-wave follow-up campaign occurred during FAST 23, in response to an early-warning notice for the candidate event S230810af. This notice was distributed at 10:01:02 UT on 2023 August 10, and was targeted for observation 27 s later, at 10:01:29 UT. Observations continued until 10:38:48 UT, when a retraction notice was sent, as the candidate was likely due to a noise transient (GCN 34378; Ligo Scientific Collaboration, VIRGO Collaboration & Kagra Collaboration 2023). FAST 24 occurred during the gap between O4a and O4b and so no GW follow-up was performed. As GRB and GW follow-up was given a higher scheduling priority than the FAST surveys, they were not directly impacted by the running of the surveys.

3.2 Classifications

The GOTO–FAST programme reported a total of 51 source classifications between its first two observing runs. Of these, 48 were extragalactic transients, two were classified as outbursts from cataclysmic variable (CV) systems, and one showed only galaxy lines within its spectrum. In addition, two sources were classified as CVs without their discovery being reported to the TNS. The majority of Galactic contaminants were identified during the vetting stage, primarily by the existence of pre-eruption sources in imaging from GOTO and other surveys. The number of transients classified as each type and subtype is shown in Fig. 5 and a complete list of classified targets and their classifications is provided in Table A1. All but one of the 48 classified extragalactic transients were classified as supernovae, with 33 being of type I, 11 of type II, and 3 identified as likely to be supernovae, but of an undetermined type. The exception is TDE 2024bgz, which was discovered by ZTF and classified during FAST 24 as a tidal disruption event.

The 31 SNe classified as either type Ia or a related subtype make up 60.8 per cent of the total number of classified sources, and 64.6 per cent of the classified extragalactic transients, when excluding CVs and the one galaxy spectrum. There are 13 classified core-collapse supernovae (CCSNe), corresponding to 25.5 and 27.1 per cent of classified sources and extragalactic transients, respectively. These fractions can be compared to those found by other magnitude limited surveys, such as the ZTF–BTS statistical sample (D. A. Perley et al. 2020), of which 72.5 per cent are SN Ia and 26.0 per cent are CCSNe. When looking at all classified supernovae discovered by GOTO, up until May 2026, 71.7 per cent are SN Ia and 26.8 per cent. The Ia fraction of GOTO–FAST transients is slightly smaller than that found in both the ZTF–BTS sample, and the general GOTO classification sample. This may partially be an effect of the FAST targeting strategy, which prioritized transients within nearby star-forming galaxies, though the small sample size involved makes it difficult to draw any firm

Downloaded from academic.oup.com/mnras/article/552/3/stag1848/8836714 by guest on 21 October 2026

conclusions. When comparing to a volume limited sample, such as ATLAS100 (S. Srivastav et al. 2026), we see more significant differences, as expected of a magnitude limited survey. Type Ia SNe are particularly luminous, and so are overrepresented compared to their volumetric fraction (35.4 per cent of the ATLAS100 classified subsample), while CCSNe are under-represented.

3.2.1 *Unclassified targets*

A small number of targets were unable to be confidently classified; the majority of these showed featureless spectra with the exception of host-galaxy emission and, in some cases, a blue continuum. This is an inherent difficulty of classifying transients at early times, as many classes of potentially interesting transients appear similar. During the first night a large number of targets were observed with the exposure times estimated by SIGNAL (Section 2.2). However, most of the resulting spectra were of poor quality and could not be used to provide confident classifications. Following this, exposure times were increased by a factor of $\sim$ 1.3 and observations of fainter targets were only attempted at lower airmasses. This reduced the number of observations taken per night but increased the fraction which were successfully classified.

GOTO24qj was identified as a potential target of interest in the GOTO stream during FAST 24. It appeared as a bright ($L = 16.44 \pm 0.02$ mag) source coincident with the nucleus of NGC 3623, a nearby galaxy at a distance of 14.7 ± 2.6 Mpc (E. Kourkchi et al. 2022) and was targeted for observation with the INT within an hour of discovery. However, the resulting spectrum showed only features associated with its host galaxy. Further inspection of the discovery difference image and subsequent observations showed that the initial detection was likely a residual left behind after subtracting the bright core of NGC 3623. This was discovered without the source being reported to the TNS, so it was not assigned an IAU name. The number of similar false-positive sources was low, with 4 targeted across both runs as well as GOTO24qj. Three of these required blind offsetting and resulted in a traceless spectrum, while one (GOTO24ni) was aborted prior to observation due to non-detection in acquisition images. The three that received a spectrum are not clearly subtraction artefacts, but were not detected in subsequent GOTO observations. GOTO24ni was later identified as a detection of JWST, albeit at a much brighter magnitude ($L \sim 14.5$ mag) than is typical in GOTO images ($L \sim 17$ mag).

3.2.2 *Time to first spectrum*

A key goal of GOTO–FAST was minimizing the delay between the discovery of a transient and spectroscopic observations. Overall this was successful, with the majority of primary targets being observed within 2 d of discovery, and a subset observed within hours. In the following analysis, we define the discovery time as the midpoint of the first observation reported to the TNS, or, for candidates which were identified in the GOTO stream but not reported, the midpoint of the first GOTO observation in which they are detected. The time of first spectrum is defined as the start of the first spectroscopic observation obtained by GOTO–FAST. The time-to-spectrum, t_s, is the difference between these two times.

A histogram of the time between discovery and the first spectral observations for all transients classified during FAST 23 and 24 is shown in Fig. 6. The targets are split into two groups, those that were discovered by GOTO, and those reported to the TNS by other surveys which were selected as secondary targets. There were 7 primary targets observed during FAST 23, with an additional 15 sources being selected from the TNS. During FAST 24, this increased to 12 primary targets, with an additional 17 secondary targets. For sources discovered by GOTO, the median time to spectrum was 1.92 d, with six being observed within a day of discovery. For secondary targets, the median was 5.78 d.

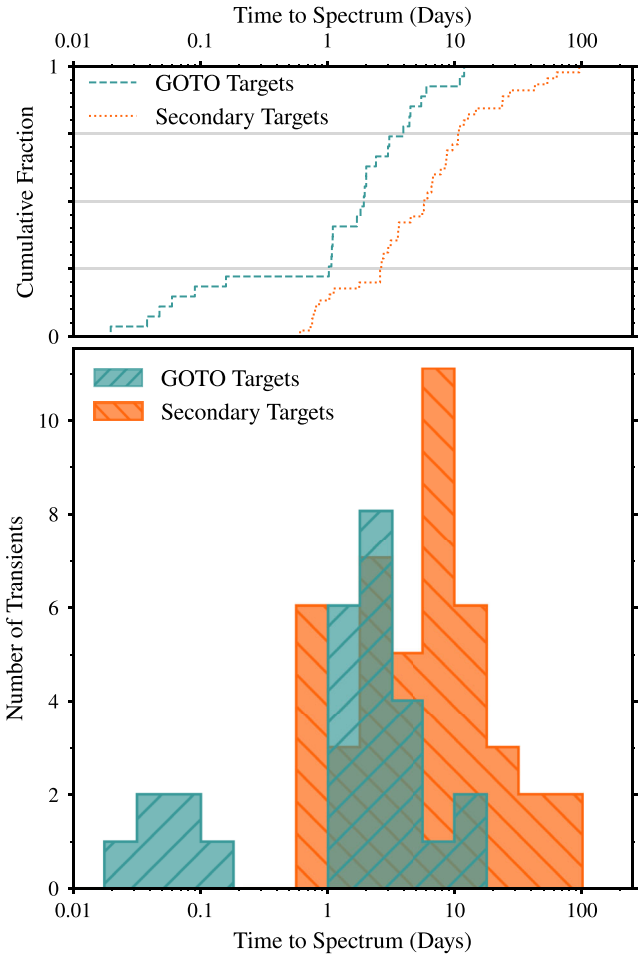


Figure 6. Histogram and cumulative distribution of the time to spectrum for GOTO-discovered and secondary targets across both GOTO–FAST observing runs.

The time-to-spectrum (t_s) is made up of two components: the time-to-vetting (t_v) between a target's discovery observation and when it is identified as a transient in the GOTO Marshall, and the time between a target being identified to being observed with the INT. These are shown in Fig. 7 and detailed in Table 5.

There are two distinct clusters, transients with $t_v < 1$ h and $t_s < 2$ h which correspond to those with latencies less than one day identified above, and those with $t_s > 24$ h. Targets which were vetted soon after discovery imaging typically received a spectrum within an hour of vetting. These represented the best opportunity for obtaining spectra at early times and so were prioritized for follow-up. The main sources of delay in these cases were waiting for the prior observation to finish, typically on the order of 30 min, and acquiring the source which typically took 5–10 min. An example of such a case is shown in Fig. 2.

Downloaded from academic.oup.com/mnras/article/552/3/stag1848/8836714 by guest on 21 October 2026

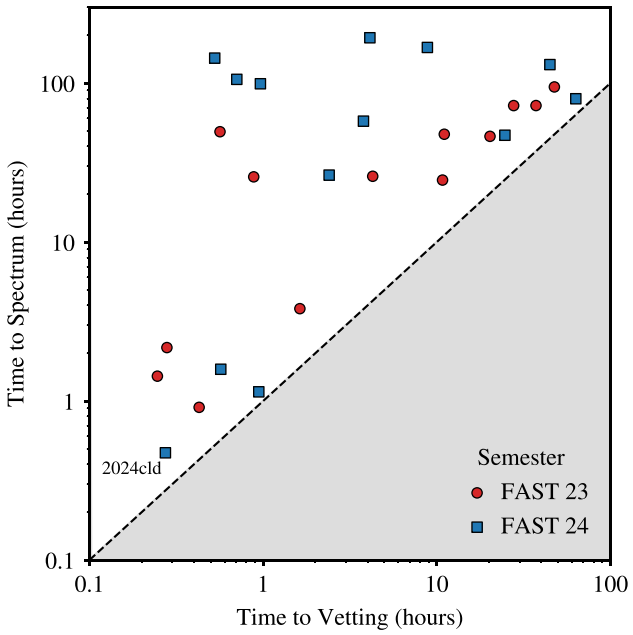


Figure 7. Interval between the time of discovery (the mid-point of the discovery observation) of each GOTO–FAST primary target and the times it was human-vetted (*x*-axis) and the first spectrum was observed (*y*-axis). Targets from FAST 23 and FAST 24 are shown as red circles and blue squares, respectively. A dashed diagonal line shows the lower bound where $t_s = t_v$.

Prior to FAST 23 it was believed that we could carry out immediate observation of any transient discovered by GOTO-N during the night, however, it became clear this would not be possible. As discussed in Section 3.2.1, our initial exposure time and SNR estimates were optimistic, and in reality it was difficult and time consuming to classify targets fainter than $L \approx 19$ mag. This meant that for the majority of GOTO discoveries there was an unavoidable delay while waiting for them to brighten enough to observe. The use of a more sensitive spectrograph, capable of classifications down to $L = 20$ mag, would mostly negate this source of delay. Faint targets did still benefit from the high-cadence survey due to the ability to target them as soon as they were bright enough to observe with IDS.

3.3 Selected transients

Between FAST 23 and 24, a number of peculiar transients were identified which warranted further follow-up. Here, we detail a few such transients, however this list is not intended to be exhaustive or a complete description of each object. We refer the interested reader to the relevant follow-up paper where it exists.

3.3.1 SN 2024cld

SN 2024cld (GOTO24ql) was discovered by GOTO-N as part of the FAST 24 survey at 05:29 UT on 2024 February 13 (M. Pursiainen et al. 2024) within NGC 6004, an intermediate spiral galaxy (G. Vaucouleurs et al. 1991) at a distance of 41.5 ± 0.2 Mpc (R. B. Tully et al. 2013). Upon ingestion to the Marshall, it was immediately identified as a high priority target by the observers and spectroscopic observations began with the INT just 28 min after discovery, as shown in Figs 2 and 7.

Table 5. Time to vetting (t_v) and spectrum (t_s) for classified GOTO–FAST targets that were discovered by GOTO.

Semester	TNS name	GOTO name	t_v (h)	t_s (h)
FAST 23	2023oun	GOTO23vp	27.74	72.29
	2023oxa	GOTO23wf	37.30	72.32
	2023oza	GOTO23yj	0.25	1.43
	2023pgr	GOTO23aan	10.80	24.58
	2023pnt	GOTO23aaz	0.88	25.75
	2023pso	GOTO23ur	0.56	49.50
	2023psp	GOTO23adr	1.63	3.81
	2024bci	GOTO24gy	8.84	167.81
FAST 24	2024bfu	GOTO24ih	0.71	105.71
	2024biz	GOTO24lw	3.78	57.69
	2024bjb	GOTO24mr	63.26	79.80
	2024bqu	GOTO24jz	0.97	99.17
	2024bth	GOTO24na	2.40	26.41
	2024bto	GOTO24hl	4.12	193.10
	2024bvg	GOTO24nz	24.71	47.05
	2024bvh	GOTO24mq	44.88	130.92
	2024bww	GOTO24oj	0.53	143.82
	2024bzq	GOTO24pj	0.57	1.59
	2024cld	GOTO24ql	0.27	0.47

At discovery, SN 2024cld had an *L*-band magnitude of 17.956 ± 0.076 mag, with a non-detection 23 h earlier to a 5σ limit of $L > 18.943$ mag. The initial spectrum (B. Godson et al. 2024c) showed strong flash ionization features, dominated by H and He emission lines with narrow peaks and broad wings. The discovery and classification of SN 2024cld as a young, flash-ionized, type II supernova within a nearby galaxy was highlighted in an AstroNote (B. Warwick et al. 2024), to encourage further follow-up by the wider community.

Two additional spectra of 2024cld were obtained with the INT: the first at +1.4 d post-explosion (≈ 1 d post-discovery) during FAST 24, and the second at +15.3 d, using the higher dispersion R400V grating, as part of the payback time allocated to the programme due to a dome fault which caused the loss of one night. Four spectra were also obtained with LT/SPRAT at +3.5, +7.4, +11.3, and +12.3 d, respectively.

After the conclusion of FAST 24, follow-up photometry, spectroscopy, and polarimetry was continued using a wide range of facilities. A complete description of these observations and the first year of evolution of SN 2024cld is provided by T. L. Killestein et al. (2025a). Their favoured interpretation is that of an evolved supergiant star, surrounded by a multi-component CSM consisting of a dense disc and tenuous wind-like structure resulting from extreme mass transfer in the final centuries before explosion. The flash-ionization features of early time spectra obtained by GOTO–FAST were key to constraining the structure of the CSM close to the progenitor, and therefore its mass-loss history during its terminal years.

Observations of 2024cld are ongoing, over two years from its first detection. At its current brightness ($r \sim 21.5$ mag) it is accessible photometrically to 2.5 m class telescopes and spectroscopically to 8 m class telescopes. *JWST* observations obtained in July 2026 are hoped to constrain dust emission, which has not been evident in *JHK*-band measurements up to this point.

Downloaded from academic.oup.com/mnras/article/552/3/stag1848/8836714 by guest on 21 October 2026

3.3.2 SN 2024bfu

SN 2024bfu was discovered on 2024 January 31 as part of the FAST 24 survey (B. Godson et al. 2024b) and was classified within a day of discovery as a type Iax supernova (R. Brivio et al. 2024) by the advanced Public ESO Spectroscopic Survey for Transient Objects (ePESSTO+; S. J. Smartt et al. 2015). Type Iax SNe are a peculiar subclass of thermonuclear supernovae, with much lower ejecta velocity and luminosities than normal type Ia SNe (R. J. Foley et al. 2013). The leading model to explain their properties is that of a helium-accreting white dwarf undergoing a deflagration explosion which does not necessarily unbind the whole star (e.g. G. C. Jordan et al. 2012; M. Kromer et al. 2013). However, many alternative models exist (e.g. R. Fernández & B. D. Metzger 2013; M. D. Stritzinger et al. 2015; F. P. Callan et al. 2024), and there is significant observational diversity within this class which is not yet fully understood. Two epochs of spectroscopy were obtained of 2024bfu as part of FAST 24 which are presented alongside GOTO photometry and data from other facilities in M. R. Magee et al. (2025).

3.3.3 SN 2024cew

SN 2024cew was discovered as part of GOTO's response to GRB 240209A (S. Belkin et al. 2024), a long GRB detected by the *Fermi* GBM at 06:19:19.82 UT on 2024 February 09 (Fermi GBM Team 2024). 2024cew was discovered at 05:27 UT on 11 February (1.96 d post trigger) with a magnitude of $L = 19.64 \pm 0.14$. It was detected again ~ 22 h later (2.9 d post trigger) at $L = 20.45 \pm 0.19$ mag. This power-law decline, with an index of -1.80 ± 0.16, is consistent with a GRB afterglow, and it was the only candidate optical counterpart within the 90 per cent GBM localization region. Observations taken the next night at the Nordic Optical Telescope (A. Ugarte Postigo et al. 2024) showed that the source had brightened, reaching $r = 19.80 \pm 0.05$ mag, additional observations from Wendelstein Observatory corroborated this and showed an additional rise to $r = 19.5 \pm 0.1$ mag (M. Busmann et al. 2024). Following this re-brightening, 2024cew was targeted for observation with the INT and a spectrum was obtained at 05:10 UT on 2024 February 14 (B. Godson et al. 2024a). The spectrum was consistent with a type Ia SN at a redshift of z = 0.15, though there were also weaker matches to templates of a 91T-like SN (A. V. Filippenko et al. 1992), and it was classified as a type Ia-pec. This classification means it is unlikely to be related to GRB 240209A (K. Ackley et al. 2024). The spectrum of 2024cew also matches to templates of SN 2000cx, a very peculiar Ia with a spectrum similar to that of 91T-like SN, but with prominent Fe III features visible weeks post-peak and a very unusual photometric evolution (W. Li et al. 2001; J. M. Silverman et al. 2013). At the measured redshift, both the initial detection and the re-brightening correspond to absolute magnitudes of around -19.6 (assuming $H_0 = 70\,\mathrm{km\,s^{-1}\,Mpc^{-1}}$ in a flat universe with $\Omega_m = 0.3$). Bright, short-lived, early emission has been observed in some peculiar SNe Ia, especially transitional, or hybrid, 02es-like SNe (see J.-A. Jiang et al. 2017) such as SN 2019yvq (A. A. Miller et al. 2020; J. Burke et al. 2021; M. A. Tucker et al. 2021), SN 2022vqz (G. Xi et al. 2024), and a particularly bright excess seen in SN 2022ywc (S. Srivastav et al. 2023). Compared to these examples, the initial excess observed in 2024cew is very bright and the time-scale of its decay and subsequent re-brightening is very fast. Unfortunately, we have little photometric data of 2024cew after its re-brightening, and only a single, low S/N spectrum, which makes any further study of this event difficult.

3.3.4 TDE 2022dbl

TDE 2022dbl is an optical tidal disruption event which was first discovered by ASAS-SN on 2022 February 22. During the course of FAST 24, a second flare from 2022dbl was detected by ZTF (Y. Yao et al. 2024), and was targeted for follow-up by GOTO–FAST. We observed 2022dbl at 04:35 UT on 2024 February 06, providing some of the earliest spectra of the second flare. These spectra, alongside other data, were used by L. Makrygianni et al. (2025) to show that the initial flare was likely caused by the partial disruption of a star and therefore that even some typical TDEs can be caused by partial disruptions.

3.4 Comparison with TNS

To compare the performance of GOTO–FAST with other transient classification programmes, we calculated the spectral delay for all spectroscopically classified transients on the TNS which were discovered between the start of 2023 and end of 2024. For each classified transient with at least one publicly available spectrum, we used the observation time from the first spectrum on the Weizmann Interactive Supernova Data Repository (WISeREP; O. Yaron & A. Gal-Yam 2012) and the discovery date reported on the TNS to determine the time between discovery and first spectrum. There are some issues with this approach; the reported discovery date often does not necessarily reflect the earliest detection of a transient as precovery from earlier images is a common practice once a transient has been discovered.

This spectral delay distribution is shown in Fig. 8 along with the distribution of the discovery magnitudes for these sources. A small number of transients ($\sim$350) have publicly available spectra that were taken before the first observation reported to the TNS, primarily from the ZTF Spectral Energy Distribution Machine (SEDM; N. Blagorodnova et al. 2018), resulting in a negative delay using this method. These transients are not displayed on the logarithmically scaled histogram, but are included in the cumulative distribution and further analysis.

The median time to spectrum is 9.08 d, with an approximately log-normal distribution. There is also a daily modulation with peaks at an integer number of days after discovery. We attribute this to the fact that the majority of classifications are made by telescopes at longitudes similar to those that discovered the transient, in particular SEDM spectra of ZTF discovered transients. This time-scale is sufficient for the classification of typical supernovae, but is long compared to the decay time of more exotic transients like kilonovae and LFBOTS.

In comparison, the median delay for primary GOTO–FAST targets was 1.92 d, which corresponds to the 11th percentile of the TNS distribution. The target with the shortest delay (SN 2024cld/GOTO24ql) received its first spectrum faster than 98.4 per cent of classified transients.

Over the past decade, the median time to spectrum has roughly doubled. For transients discovered in 2016 the median time to spectrum is 4.6 d, while for those discovered in 2025 the median is 9.3 d. For those discovered between January and April 2026, the value is 10.3 d. In the same time-frame, the median discovery magnitude has increased over a magnitude, from 18.08 in 2016 to 19.45 in 2026. This represents the dramatic improvements to

Downloaded from academic.oup.com/mnras/article/552/3/stag1848/8836714 by guest on 21 October 2026

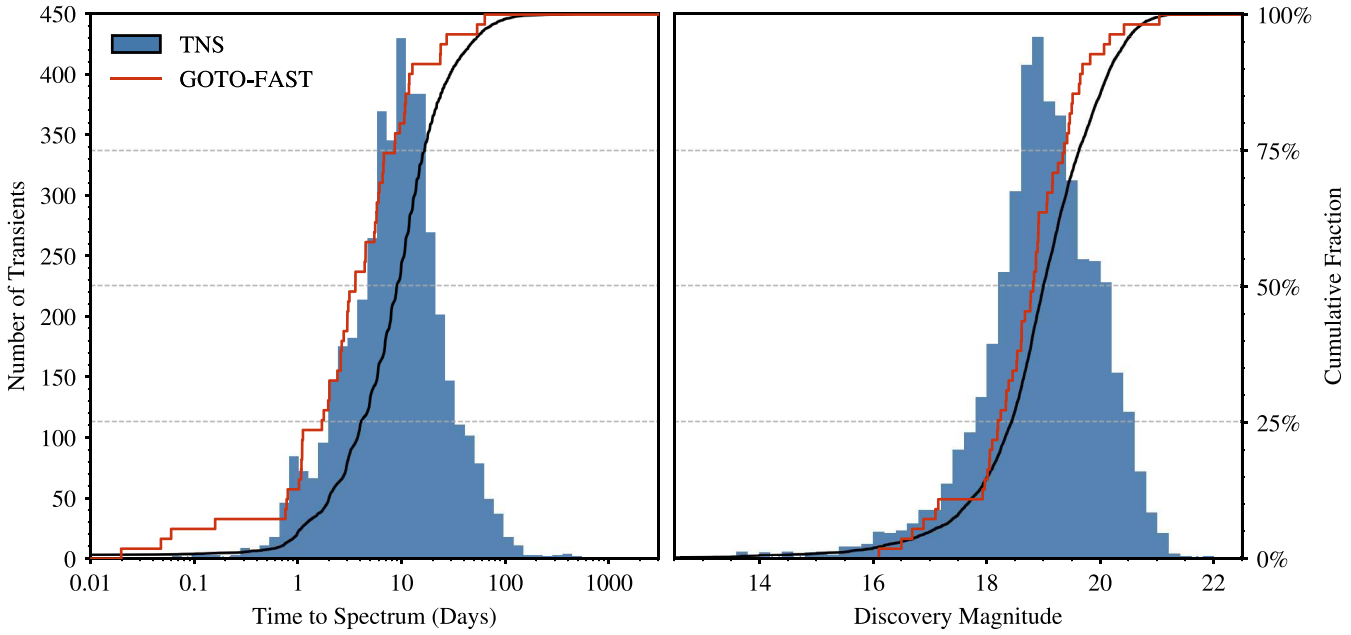


Figure 8. Left: Histogram and empirical cumulative distribution function (eCDF) of the time in days between the discovery and earliest public spectroscopic observation for all classified sources on the TNS discovered between January 2023 and December 2024. The eCDF of time-to-spectrum for GOTO–FAST classifications is also shown as a stepped line. **Right**: Histogram and eCDF of discovery magnitude for the same sources.

the depth and volume searched by discovery surveys, but also shows that our ability to promptly classify a large proportion of transients has not increased at the same rate. GOTO–FAST and similar programmes can help bridge this gap. Whilst dedicated programmes targeting a relatively small number of transients are not directly comparable to the overall TNS classification population, they do provide an opportunity to study a phase of transient evolution which is often missed.

4 CONCLUSIONS & FUTURE WORK

We have presented the results of the first two GOTO–FAST observing runs and demonstrated the effectiveness of combining a high-cadence wide-field optical survey with real-time spectroscopic follow-up.

It is possible to shift the distribution of the time-to-spectrum to significantly faster time-scales than the current TNS average, with a same-night spectroscopy for the majority of transients and a sub-hour delay for those which are immediately bright enough for spectroscopy. In the best case, we were able to identify and follow-up on novel GOTO transients within 15 min of the end of discovery imaging. In doing so we identified a number of interesting transients, and obtained spectroscopic observations of much earlier phases than would otherwise be possible. Our dataset on SN 2024cld in particular is seen as an excellent example of the utility of this programme. However, a large number of the transients classified by this programme still had significant delays in obtaining their first spectrum. While some of these delays were unavoidable, due to weather or scheduling constraints, others could be significantly improved by reducing the time between shutter close and vetting.

Since the start of this programme a number of fully automated triggering systems have begun operation, for example BTSbot (N. Rehemtulla et al. 2024) running on the ZTF stream and the GOTO Auto-Trigger (GOAT; J. D. Lyman et al. 2026), which can request observations from pt5m and the LT without human intervention. These are very efficient, and effective at identifying bright transients, but still fall behind human vetting when it comes to the purity of selected sources, especially at fainter magnitudes (see section 4 of N. Rehemtulla et al. 2024). Currently, automated trigger systems are very effective when paired with robotic follow-up facilities, like the LT and SEDM, at reducing the delay between the ingestion of a source and its identification as a genuine transient. This is an important aspect of reducing the average time to spectrum. However, when attempting to target the earliest phases of transient evolution, either dedicated time or high-priority ToO triggering is necessary and their reduced purity means there is still a benefit to target selection being performed by human vetters.

Both FAST 23 and 24 utilized a fairly resource intense dedicated visitor mode campaign, with a minimum of three observers present at the telescopes and ~ 10 others providing daytime support. The introduction of rapid response modes to target-of-opportunity triggers provide similar low-latency capabilities at a lower cost if candidates can be promptly identified and triggers are given sufficient priority. The 2.56 m Nordic Optical Telescope's (NOT) rapid-response mode for example would be well suited to a GOTO–FAST style programme, given the excellent sensitivity of the Alhambra Faint Object Spectrograph and Camera (ALFOSC) spectroscopy and co-location at the ORM.

There is significant cost involved in visitor-mode observing compared to remote or queue scheduled observations, both monetarily and in terms of the environmental impact of international travel.[4] Given these downsides, there is an overall trend in modern astronomy away from visiting observers as more telescopes

[4]We estimate the CO_2 emission from round trip flights between Birmingham, UK and Santa Cruz de La Palma as ~ 420 kg per person using version 13.1 of the ICAO Carbon Emissions Calculator.

Downloaded from academic.oup.com/mnras/article/552/3/stag1848/8836714 by guest on 21 October 2026

are roboticized and more systems are automated, including the INT itself. One benefit of visitor and remote mode programmes is the training opportunity provided to students and early career researchers in observational astronomy. Between the first two GOTO–FAST runs, a total of five PhD students and three post-doctoral researchers were trained to observe with the INT, which has a long history training the next generation of observers through both its research activities and studentship programme. For most of these students, this was their first experience observing at a >2-metre class telescope, and many of them have now taken part in other spectroscopic observation programmes, such as ePESSTO+.

Fully understanding the nature of transient objects requires observations across all phases. During GOTO–FAST we leveraged a number of facilities at the ORM to provide follow-up of transients immediately following the end of the INT run. Most of these observations relied on a large number of unrelated proposals targetting various classes of transients. Future observing runs would also benefit from coordinated observing programmes with other telescopes suited to following GOTO–FAST transients after peak as they fade and later in nebular phases. Although the INT is now unavailable for similar programmes in its new role as the host of the HARPS3 spectrograph, there is an abundance of facilities both at the ORM and beyond which are suitable for extensions of the GOTO–FAST programme. Additional observing runs are planned or have been executed at the 2.2 m telescope at Calar Alto observatory (B. Godson et al. 2025) and the Nordic Optical Telescope (M. Pursiainen et al. 2025; D. O'Neill et al. 2026).

ACKNOWLEDGEMENTS

We thank the staff of the Isaac Newton Group for their support in obtaining our spectroscopic data, and in particular the student support astronomer for our first observing run, Kellie de Vos, for providing training to our observing team at the INT. BG would additionally like to thank the staff of the ING for the in-depth training provided on the INT as part of their studentship, which overlapped with FAST 24. We would also like to thank the reviewer for their suggested revisions, and for pointing out the similarities between SN 2024cew and a number of other transients, which substantially improved the quality of the corresponding section. The Gravitational-wave Optical Transient Observer (GOTO) project acknowledges the support of the Monash–Warwick Alliance; University of Warwick; Monash University; University of Sheffield; University of Leicester; Armagh Observatory & Planetarium; the National Astronomical Research Institute of Thailand (NARIT); Instituto de Astrofísica de Canarias (IAC); University of Portsmouth; University of Turku; University of Birmingham; and the UK Science and Technology Facilities Council (STFC, grant numbers ST/T007184/1, ST/T003103/1, and ST/Z000165/1).

IDS spectroscopy was obtained under the 2023P08 and 2024P07 programmes on the Isaac Newton Telescope. The Isaac Newton Telescope is operated on the island of La Palma by the Isaac Newton Group of Telescopes in the Spanish Observatorio del Roque de los Muchachos of the Instituto de Astrofísica de Canarias.

BG, BW, and MAM acknowledge the UK Research and Innovation's STFC studentship grant funding, project reference ST/X508871/1. BDRD was supported by an STFC studentship (Ref: 2881369). DMS acknowledges support through the Ramón y Cajal grant RYC2023-044941, funded by MCIU/AEI/10.13039/501100011033 and FSE+. SM, and RS acknowledge The Leverhulme Trust grant RPG-2023-240. VSD is supported by a Leverhulme Research Fellowship (RF-2025-297/9) and the Spanish Ministry of Science, Innovation and Universities (PID2023-151588NB-I00). SM acknowledges financial support from the Research Council of Finland project 350458. AS acknowledges the Warwick Astrophysics PhD prize scholarship made possible thanks to a generous philanthropic donation. TLK acknowledges a Warwick Astrophysics prize post-doctoral fellowship made possible thanks to a generous philanthropic donation. DLC acknowledges support from the Science and Technology Facilities Council (STFC) grant number ST/X001121/1.

DATA AVAILABILITY

Unprocessed spectra and relevant calibration data are available via the Isaac Newton Group Archive, which is maintained as part of the CASU Astronomical Data Centre at the Institute of Astronomy, Cambridge. The relevant programme references are given in Table 2. Classification spectra are available on the Transient Name Server and the Weizmann Interactive Supernova Data Repository (WISeREP).

REFERENCES

Aartsen M. G. et al., 2017, Astropart. Phys., 92, 30
Abbott B. P. et al., 2020, Living Rev. Relativ., 23, 3
Ackley K. et al., 2024, GRB Coord. Netw., 35730, 1
Ahumada T. et al., 2023, Transient Name Serv. AstroNote, 349, 1
Andrews J. E. et al., 2021, ApJ, 917, 63
Angelini L., Cenko S. B., Kennea J. A., Siegel M. H., Barthelmy S. D., 2022, in Bambi C., Santangelo A., eds, Handbook of X-ray and Gamma-ray Astrophysics. Springer Nature, Singapore, p. 1
Becker A., 2015, Astrophysics Source Code Library, record ascl:1504.004
Belkin S. et al., 2024, GRB Coord. Netw., 35715, 1
Belkin S. et al., 2026, MNRAS, 550, stag1193
Bellm E. C. et al., 2018, PASP, 131, 018002
Benn C., 2014, Exposure Time Calculator–SIGNAL, Isaac Newton Group of Telescopes, Santa Cruz de La Palma, Spain
Blagorodnova N. et al., 2018, PASP, 130, 035003
Blaufuss E., Kintscher T., Lu L., Tung C. F., 2019, The Next Generation of IceCube Realtime Neutrino Alerts. preprint (arXiv:1908.04884)
Blondin S., Tonry J. L., 2007, ApJ, 666, 1024
Bostroem K. A. et al., 2023, ApJ, 956, L5
Bowler S., 2025, Astron. Geophys., 66, 1
Brivio R., Ferro M., Benetti S., Yaron O., 2024, Transient Name Serv. Classif. Rep., 2024–315, 1
Bruch R. J. et al., 2023, ApJ, 952, 119
Burke J. et al., 2021, ApJ, 919, 142
Busmann M., Gruen D., O'Connor B., Palmese A., Hu L., Riffeser A., 2024, GRB Coord. Netw., 35724, 1
Callan F. P. et al., 2024, MNRAS, 530, 1457
Cao Z., Jonker P. G., Wen S., Zabludoff A. I., 2024, A&A, 691, A228
Chambers K. C. et al., 2016, The Pan-STARRS1 Surveys, preprint (arXiv:1612.05560)
Colombo A., Salafia O. S., Gabrielli F., Ghirlanda G., Giacomazzo B., Perego A., Colpi M., 2022, ApJ, 937, 79
de Ugarte Postigo A., Malesani D. B., Andersen M. I., Sollerman J., 2024, GRB Coord. Netw., 35716, 1
de Vaucouleurs G., de Vaucouleurs A., Corwin Jr H. G., Buta R. J., Paturel G., Fouque P., 1991, Third Reference Catalogue of Bright Galaxies. 1 Vol. 1, Springer-Verlag, Berlin
Drout M. R. et al., 2014, ApJ, 794, 23

Downloaded from academic.oup.com/mnras/article/552/3/stag1848/8836714 by guest on 21 October 2026

Dyer M. J., 2020, Phd thesis Univ. Sheffield
Dyer M. J. et al., 2020, in Proc. SPIE Conf. Ser. Vol. 11445, Ground-Based and Airborne Telescopes VIII. SPIE, Bellingham, p. 157
Dyer M. J. et al., 2024, Proc. SPIE Conf. Ser. Vol. 2024, The Gravitational-wave Optical Transient Observer (GOTO). SPIE, Bellingham, p. 8
Fathivavsari H., Domínguez-Palmero L., Hardy L., Méndez J., 2013, Arc Maps for the CuAr and CuNe Lamps When Used with IDS/Red+2
Fausnaugh M. M. et al., 2021, ApJ, 908, 51
Fausnaugh M. M. et al., 2023, ApJ, 956, 108
Fermi GBM Team, 2024, GRB Coord. Netw., 35712, 1
Fernández R., Metzger B. D., 2013, ApJ, 763, 108
Filippenko A. V. et al., 1992, ApJ, 384, L15
Foley R. J. et al., 2013, ApJ, 767, 57
Förster F. et al., 2016, ApJ, 832, 155
Fremling C. et al., 2020, ApJ, 895, 32
Gal-Yam A. et al., 2014, Nature, 509, 471
Gillan A. F. et al., 2026, Time-Domain Photometry and Activity Evolution of Interstellar Comet 3I/ATLAS with BHTOM, preprint (arXiv:2603.01383)
Godson B. et al., 2023, Transient Name Serv. AstroNote, 224, 1
Godson B. et al., 2024a, Transient Name Serv. AstroNote, 52, 1
Godson B. et al., 2024b, Transient Name Serv. Discovery Rep., 2024–300, 1
Godson B. et al., 2024c, Transient Name Serv. Classif. Rep., 2024–429, 1
Godson B., Palau C. J., Pursiainen M., Magee M., Lyman J., Galbany L., Killestein T., 2025, Transient Name Serv. Classifi. Rep., 2025–1195, 1
Gompertz B. et al., 2020, MNRAS, 497, 726
Groot P. J. et al., 2024, PASP, 136, 115003
Gutiérrez C. P. et al., 2024, ApJ, 977, 21
Hardy L. K., Butterley T., Dhillon V. S., Littlefair S. P., Wilson R. W., 2015, MNRAS, 454, 4316
Hinds K. et al., 2026, Transient Name Serv. AstroNote, 43, 1
Hinkle J. T. et al., 2025, Sci. Adv., 11, eadt0074
Ho A. Y. Q. et al., 2023, ApJ, 949, 120
Ivezić {. et al., 2019, ApJ, 873, 111
Jacobson-Galán W. V. et al., 2022, ApJ, 932, 58
Jiang J.-A. et al., 2017, Nature, 550, 80
Jones D. O. et al., 2021, ApJ, 908, 143
Jordan G. C., Perets H. B., Fisher R. T., van Rossum D. R., 2012, ApJ, 761, L23
Khamrat S. et al., 2026, Universe, 12, 53
Khazov D. et al., 2016, ApJ, 818, 3
Killestein T. L. et al., 2021, MNRAS, 503, 4838,
Killestein T. L. et al., 2024, MNRAS, 533, 2113
Killestein T. L. et al., 2025a, MNRAS, 548, 24
Killestein T. L. et al., 2025b, A&A, 699, A8
Kochanek C. S., 2019, MNRAS, 483, 3762
Kongsathitporn N. et al., 2024, PASP, 136, 124507
Kourkchi E., Tully R. B., Courtois H. M., Dupuy A., Guinet D., 2022, MNRAS, 511, 6160
Kromer M. et al., 2013, MNRAS, 429, 2287
Kumar A. et al., 2025, MNRAS, 544, 47
Law N., Soto A. V., Corbett H., Galliher N., Gonzalez R., Machia L., Walters G., 2022, in Proc. SPIE Conf. Ser. Vol. 9147, Ground-Based and Airborne Telescopes IX. SPIE, Bellingham, p. 16
Law N. M. et al., 2022, PASP, 134, 035003
Li W. et al., 2001, PASP, 113, 1178
Ligo Scientific Collaboration, VIRGO Collaboration, Kagra Collaboration, 2023, GRB Coord. Netw., 34378, 1
Lyman J. D. et al., 2026, RAS Tech. Instrum., 5, rzag042
Magee M. R. et al., 2025, MNRAS, 543, 3731
Makrygianni L. et al., 2025, ApJ, 987, L20
Miller A. A. et al., 2020, ApJ, 898, 56
Moriya T. J., Menon A., 2024, PASJ, 76, L27
Müller-Bravo T. E., 2023, Temuller/Idsred: First Release!, Zenodo
O'Neill D. et al., 2026, GRB Coord. Netw., 44914, 1
Ofek E. O., Ben-Ami S., 2020, PASP, 132, 125004
Ofek E. O. et al., 2023, PASP, 135, 065001
Pastorello A. et al., 2019, A&A, 630, A75
Perley D. A. et al., 2020, ApJ, 904, 35
Piascik A. S., Steele I. A., Bates S. D., Mottram C. J., Smith R. J., Barnsley R. M., Bolton B., 2014, in Proc. SPIE Conf. Ser. Vol. 9147, Ground-Based and Airborne Instrumentation for Astronomy V.. SPIE, Bellingham, p. 91478H
Prentice S. J. et al., 2018, ApJ, 865, L3
Prochaska J. X. et al., 2020a, Pypeit/PypeIt: Release 1.0.0, Zenodo
Prochaska J. X. et al., 2020b, J. Open Source Softw., 5, 2308
Pursiainen M. et al., 2018, MNRAS, 481, 894
Pursiainen M. et al., 2024, Transient Name Serv. Discovery Rep., 2024–422, 1
Pursiainen M. et al., 2025, Transient Name Serv. AstroNote, 269, 1
Ramsay G. et al., 2026, Searching for Outbursts from Symbiotic Binaries in GOTO and ATLAS Data
Rees M. J., 1988, Nature, 333, 523
Rehemtulla N. et al., 2024, ApJ, 972, 7
Ricker G. R. et al., 2015, J. Astron. Telesc. Instrum. Syst., 1, 014003
Rose S., Lau R. M., Jencson J. E., Kasliwal M. M., De K., Ressler M. E., Fox O. D., Hankins M. J., 2025, ApJ, 980, L14
Shappee B. J. et al., 2014, ApJ, 788, 48
Shun-jing YU., Francois GONZALEZ., Jian-yan WEI., Shuang-nan ZHANG., Bertrand CORDIER., 2020, Chin. Astron. Astrophys., 44, 269
Silverman J. M. et al., 2013, MNRAS, 436, 1225
Sinclair J., 1996, ING Spectrophotometric Standards (TN100). Isaac Newton Group of Telescopes, Santa Cruz de La Palma, Spain
Smartt S. J. et al., 2015, A&A, 579, A40
Srivastav S. et al., 2023, ApJ, 956, L34
Srivastav S. et al., 2026, MNRAS, 549, stag1028
Steeghs D. et al., 2022, MNRAS, 511, 2405
Steele I. A. et al., 2004, in Proc. SPIE Conf. Ser. Vol. 5489, Ground-Based Telescopes. SPIE, Bellingham, p. 679
Stone N. C., Metzger B. D., 2016, MNRAS, 455, 859
Stritzinger M. D. et al., 2015, A&A, 573, A2
Thompson D. J., Wilson-Hodge C. A., 2023, in, Handbook of X-ray and Gamma-ray Astrophysics. Springer, Singapore, p. 1
Thompson S. J. et al., 2016, in Proc. SPIE Conf. Ser. Vol. 9908, Ground-Based and Airborne Instrumentation for Astronomy VI. SPIE, Bellingham, p. 1949
Thompson T. A., Prieto J. L., Stanek K. Z., Kistler M. D., Beacom J. F., Kochanek C. S., 2009, ApJ, 705, 1364
Tonry J. L. et al., 2018a, PASP, 130, 064505
Tonry J. L. et al., 2018b, ApJ, 867, 105
Touchard-Paxton C. G. et al., 2025, MNRAS, 537, 1015
Tsuna D., Ishii A., Kuriyama N., Kashiyama K., Shigeyama T., 2020, ApJ, 897, L44
Tucker M. A. et al., 2021, ApJ, 914, 50
Tully R. B. et al., 2013, AJ, 146, 86
Valerin G. et al., 2025, A&A, 695, A43
van Velzen S., Holoien T. W.-S., Onori F., Hung T., Arcavi I., 2020, Space Sci. Rev., 216, 124
Wang T. et al., 2023, Sci. China Phys. Mech. Astron., 66, 109512
Warwick B. et al., 2024, Transient Name Serv. AstroNote, 48, 1
Xi G. et al., 2024, MNRAS, 527, 9957
Yao Y., Chornock R., LeBaron N., Hammerstein E., Ravi V., Somalwar J., Perley D., 2024, Transient Name Serv. AstroNote, 43, 1
Yaron O., Gal-Yam A., 2012, PASP, 124, 668

APPENDIX A: OBSERVATIONS AND CLASSIFICATIONS

Downloaded from academic.oup.com/mnras/article/552/3/stag1848/8836714 by guest on 21 October 2026

Table A1. Classifications reported by GOTO–FAST.

Target name	Classification	Right ascension	Declination	Discovery time (UT)	Discovery source
SN 2024cld	SN II	$15^h50^m21^s.61$	$+18°56'21''.07$	2024-02-13 05:28:40	GOTO–FAST
SN 2024cew	SN Ia-pec	$17^h01^m05^s.29$	$+68°43'46''.30$	2024-02-11 05:27:37	GOTO–FAST
AT 2024bzq	Other[1]	$11^h44^m33^s.98$	$+36°26'41''.05$	2024-02-09 10:03:27	GOTO–FAST
SN 2024bww	SN Ia	$10^h04^m28^s.73$	$+50°43'23''.90$	2024-02-07 22:12:38	GOTO–FAST
SN 2024bvg	SN Ia	$12^h30^m22^s.95$	$+10°52'19''.42$	2024-02-06 04:59:06	GOTO–FAST
SN 2024bqu	SN Ia	$10^h55^m59^s.10$	$+11°54'56''.24$	2024-02-05 00:26:10	GOTO–FAST
SN 2024bth	SN IIn	$07^h18^m38^s.25$	$+04°18'35''.54$	2024-02-04 22:04:22	GOTO–FAST
SN 2024bvh	SN Ia	$05^h42^m10^s.47$	$+10°36'24''.75$	2024-02-02 11:19:58	GOTO–FAST
SN 2024biz	SN IIP	$05^h14^m32^s.95$	$-04°40'33''.12$	2024-02-02 10:33:48	GOTO–FAST
SN 2024bjb	SN Ia-91bg-like	$11^h11^m55^s.80$	$+03°08'01''.37$	2024-01-31 13:16:33	GOTO–FAST
SN 2024bto	SN Ia	$15^h11^m03^s.58$	$+07°31'50''.14$	2024-01-27 06:13:07	GOTO–FAST
SN 2024bci	SN Ia	$13^h37^m24^s.54$	$+27°25'10''.23$	2024-01-24 05:30:21	GOTO–FAST
SN 2023psp	SN Ia	$19^h40^m29^s.35$	$+58°24'11''.00$	2023-08-17 21:51:31	GOTO–FAST
SN 2023pnt	SN IIP	$00^h01^m57^s.48$	$+09°53'19''.55$	2023-08-14 01:19:50	GOTO–FAST
SN 2023pgr	SN	$23^h47^m33^s.20$	$+16°58'16''.91$	2023-08-13 00:19:45	GOTO–FAST
SN 2023oza	SN Ia	$17^h00^m59^s.85$	$+22°40'10''.05$	2023-08-10 20:54:08	GOTO–FAST
SN 2023oun	SN Ia	$04^h53^m13^s.69$	$+63°10'10''.45$	2023-08-08 04:02:41	GOTO–FAST
SN 2023oxa	SN Ia	$13^h41^m48^s.70$	$+26°23'28''.68$	2023-08-07 21:12:48	GOTO–FAST
SN 2023pso	SN Ib	$23^h36^m14^s.33$	$+02°09'17''.11$	2023-08-07 00:45:50	GOTO–FAST
SN 2024cdt	SN II	$15^h20^m42^s.90$	$+49°06'26''.47$	2024-02-11 10:30:43	ZTF
SN 2024cmh	SN Ia	$13^h01^m29^s.20$	$+07°50'29''.55$	2024-02-11 08:54:14	ZTF
SN 2024bio	SN Ia	$10^h24^m49^s.98$	$+28°41'08''.42$	2024-02-01 06:09:09	ZTF
TDE 2024bgz	TDE	$09^h44^m04^s.76$	$-04°12'04''.89$	2024-02-01 06:04:19	ZTF
SN 2024ccf	SN Ia	$05^h30^m27^s.41$	$-13°50'00''.20$	2024-01-31 07:03:21	ZTF
SN 2024bgg	SN Ia	$05^h26^m36^s.38$	$-10°32'50''.35$	2024-01-31 05:27:34	ZTF
SN 2024bgw	SN Ia	$03^h48^m31^s.54$	$-05°10'05''.70$	2024-01-30 06:07:12	ZTF
SN 2024bgr	SN Ia	$04^h48^m21^s.19$	$-20°25'02''.38$	2024-01-27 05:08:09	ZTF
SN 2023pnd	SN Ia	$19^h57^m34^s.14$	$+61°55'56''.79$	2023-08-15 06:18:37	ZTF
SN 2023pmv	SN Ia	$17^h58^m54^s.05$	$+36°58'47''.90$	2023-08-15 05:38:24	ZTF
SN 2023oyz	SN Ic	$17^h12^m00^s.66$	$+23°22'37''.42$	2023-08-09 05:10:06	ZTF
SN 2023owj	SN Ia	$18^h41^m59^s.98$	$+35°06'55''.98$	2023-08-08 06:52:01	ZTF
SN 2023pbh	SN Ia	$23^h57^m52^s.81$	$+12°03'50''.43$	2023-08-07 10:03:21	ZTF
SN 2023ote	SN II	$23^h44^m54^s.95$	$+12°21'21''.44$	2023-08-07 09:36:00	ZTF
SN 2023nsm	SN Ia	$23^h25^m52^s.80$	$+32°12'04''.16$	2023-07-17 08:35:52	ZTF
SN 2023meo	SN IIn	$21^h40^m59^s.12$	$+24°00'26''.29$	2023-06-24 09:44:16	ZTF
SN 2023mtp	Other[1]	$17^h14^m08^s.56$	$+81°04'29''.41$	2023-05-14 09:48:57	ZTF
SN 2024byg	SN II	$12^h51^m53^s.88$	$-04°34'24''.96$	2024-02-08 13:12:00	ASAS-SN
AT 2024cmn	Galaxy	$12^h25^m41^s.09$	$-16°37'25''.52$	2024-02-13 05:50:13	ATLAS
SN 2024bzx	SN Ia	$12^h42^m50^s.75$	$+20°41'13''.39$	2024-02-09 12:10:54	ATLAS
SN 2024brg	SN II	$03^h14^m09^s.28$	$+16°28'29''.62$	2024-02-05 06:38:46	ATLAS
SN 2024bkg	SN Ia	$13^h18^m01^s.49$	$+15°44'52''.57$	2024-02-01 13:11:55	ATLAS
SN 2024bjk	SN Ia	$15^h06^m33^s.86$	$+05°13'23''.93$	2024-01-31 14:18:35	ATLAS
SN 2024anm	SN Ia	$16^h28^m36^s.85$	$+40°56'02''.32$	2024-01-18 15:15:14	ATLAS
SN 2023zao	SN IIP	$13^h06^m23^s.41$	$+35°14'01''.28$	2023-12-06 15:15:45	ATLAS
SN 2023pjx	SN Ia	$01^h31^m25^s.59$	$+12°24'31''.21$	2023-08-14 03:05:54	ATLAS
SN 2023pbe	SN Ia	$21^h50^m39^s.98$	$+13°17'07''.30$	2023-08-12 05:43:34	ATLAS
SN 2023ozl	SN Ia	$22^h44^m12^s.56$	$+10°36'58''.78$	2023-08-10 22:41:04	ATLAS
AT 2023osr	CV	$17^h11^m11^s.12$	$+22°44'37''.73$	2023-08-07 09:22:26	ATLAS
SN 2023oqt	SN Ia	$18^h20^m40^s.20$	$+59°38'47''.05$	2023-08-06 08:57:34	ATLAS
SN 2023oxc	SN	$16^h04^m31^s.47$	$+36°19'00''.59$	2023-08-06 06:52:07	ATLAS
SN 2024btj	SN II	$11^h39^m14^s.44$	$+56°15'38''.60$	2024-02-05 23:08:07	XOSS
AT 2023nnk	CV	$17^h03^m47^s.31$	$+24°39'06''.40$	2023-07-19 17:45:03	XOSS

Note. [1] Blue continuum which could not be confidently classified. These were reported to the TNS as'Other'.

Downloaded from academic.oup.com/mnras/article/552/3/stag1848/8836714 by guest on 21 October 2026

Table A2. Spectra observed during FAST 23.

Target name	Internal name	Discovery date (MJD)	Observation date (MJD)	t_s (d)	Exposure time (s)
AT 2023pof	GOTO23vt	60164.1217	60165.9396	1.818	660
			60166.9729	2.851	3,600
			60167.0169	2.895	3,600
SN 2023oxa	GOTO23wf	60163.8839	60165.8980	2.014	1,200
SN 2023ote	GOTO23vb	60163.4000	60165.9900	2.59	1,260
AT 2023pbp	GOTO23vn	60163.4380	60166.1134	2.665	3,600
SN 2023pso	GOTO23ur	60163.0318	60166.0914	3.06	360
			60174.1213	11.08	1,800
SN 2023oza	GOTO23yj	60166.8709	60166.9146	0.0275	5,400
AT 2023ohp	AT2023ohp	60155.4340	60166.0525	10.62	1,800
SN 2023oun	GOTO23vp	60164.1685	60166.1833	2.015	360
SN 2023nsm	AT2023nsm	60142.3583	60166.1971	23.84	1,260
AT 2023mfm	AT2023mfm	60123.3990	60166.1550	42.76	1,800
			60167.0832	43.67	5,400
AT 2023oct	AT2023oct	60151.3310	60166.0242	14.69	1,800
AT 2023ozm	GOTO23zf	60167.1066	60167.1447	0.03807	3,600
AT 2023poc	GOTO23yo	60166.9115	60167.9615	1.033	5,400
AT 2023osr	AT2023osr	60163.3906	60167.9065	4.505	3,600
AT 2023otv	AT2023otv	60160.3690	60168.1420	7.773	1,800
GOTO23yp	GOTO23yp	60166.0980	60168.0492	1.929	5,230
SN 2023pbe	AT2023pbe	60168.2386	60168.9852	0.7466	2,700
			60169.0171	0.7785	2,700
GOTO23xo	GOTO23xo	60164.2239	60168.1705	3.947	3,600
SN 2023oqt	GOTO23xd	60162.3733	60168.9169	6.522	7,200
SN 2023ozo	AT2023ozo	60166.7819	60169.9304	3.138	3,600
			60170.8968	4.104	3,600
			60172.9168	6.11	5,400
			60173.9026	7.099	5,400
			60174.8995	8.097	4,341
GOTO23aak	GOTO23aak	60168.9191	60169.9685	1.049	2,700
			60170.0009	1.082	2,700
AT 2023pbg	AT2023pbg	60168.3840	60169.0880	0.6723	4,042
			60170.1311	1.747	3,305
SN 2023pgr	GOTO23aan	60169.0137	60170.0617	1.024	7,200
			60171.0598	2.025	7,200
			60172.2021	3.188	1,800
			60174.1726	5.13	6,000
			60175.1309	6.096	5,400
SN 2023oyz	GOTO23aao	60165.2153	60170.9663	5.727	7,200
AT 2023nnk	GOTO23sz	60144.7396	60171.9651	27.23	1,800
AT 2023opo	AT2023opo	60162.6962	60171.1929	8.486	3,600
SN 2023oxc	GOTO23uh	60162.2862	60171.9121	9.61	5,400
SN 2023pmv	AT2023pmv	60171.2350	60171.9915	0.7565	2,700
			60172.0243	0.7893	2,700
SN 2023pnt	GOTO23aaz	60170.0554	60171.1284	1.073	3,600
			60173.1795	3.108	5,400
SN 2023pnd	GOTO23acm	60171.2629	60172.0607	0.7978	3,600
SN 2023meo	AT2023meo	60119.4058	60172.9729	53.57	3,600
			60173.0155	53.61	3,600
GOTO23acp	GOTO23acp	60172.0635	60172.1326	0.04774	7,200
SN 2023pjx	GOTO23abu	60170.1291	60173.1325	3.003	1,800
AT 2023mtp	AT2023mtp	60078.4090	60173.9831	95.57	1,800
			60174.9673	96.56	600
SN 2023ozl	GOTO23aay	60166.9452	60173.0812	6.12	5,400
SN 2023psp	GOTO23adr	60173.9108	60174.0557	0.1309	4,800
AT 2023pjz	GOTO23acd	60170.3658	60174.0128	3.638	2,400
SN 2023pbh	GOTO23abw	60163.4190	60175.1957	11.76	3,600
SN 2023owj	GOTO23acl	60164.2861	60175.0710	10.77	3,400

Downloaded from academic.oup.com/mnras/article/552/3/stag1848/8836714 by guest on 21 October 2026

Table A2. – *continued* Spectra observed during FAST 24.

Target name	Internal name	Discovery date (MJD)	Observation date (MJD)	t_s (d)	Exposure time (s)
SN 2024bgr	2024bgr	60336.2140	60344.9131	8.681	4,500
AT 2024bfu	GOTO24ih	60340.5575	60344.9763	4.405	3,600
			60353.0525	12.48	3,600
SN 2024biz	GOTO24lw	60342.4401	60344.8581	2.404	3,600
			60345.8894	3.42	7,439
			60348.9029	6.442	5,400
			60353.8652	11.41	5,400
SN 2024bci	GOTO24gy	60333.2294	60345.1042	11.87	1,800
GOTO24nb	GOTO24nb	60343.4582	60345.9748	2.503	3,600
SN 2024bkg	GOTO24kd	60341.5500	60345.1452	3.578	4,500
SN 2024bjb	GOTO24mr	60340.5532	60345.0500	4.486	2,700
TDE 2020afhd	2020afhd	59142.4070	60346.8809	1204	1,800
SN 2024bqu	GOTO24jz	60345.0182	60346.1353	1.096	5,400
SN 2024bth	GOTO24na	60344.9197	60346.0435	1.1	6,000
SN 2024bgg	GOTO24in	60340.2275	60346.9281	6.677	6,000
TDE 2022dbl	2022dbl	59632.6200	60346.1915	713.6	1,800
			60351.0524	718.4	8,100
			60353.1529	720.5	5,400
			60354.0440	721.4	5,400
AT 2024bqo	2024bqo	60344.3902	60346.9870	2.59	2,400
			60347.0081	2.618	1,200
SN 2024bvh	GOTO24mq	60342.4722	60347.9503	5.455	6,000
TDE 2024bgz	2024bgz	60341.2530	60347.0439	5.777	3,600
			60350.9597	9.691	5,400
			60353.9749	12.71	5,400
SN 2024btj	2024btj	60345.9640	60347.1022	1.117	5,400
SN 2024bto	GOTO24hl	60336.2591	60347.2364	10.98	600
SN 2024bgw	2024bgw	60339.2550	60347.8738	8.596	6,000
AT 2024bxo	2024bxo	60348.2366	60348.8557	0.6085	2,700
SN 2024bvg	GOTO24nz	60346.2077	60348.1913	1.96	6,000
SN 2023zao	2023zao	60284.6359	60348.1342	63.48	3,600
SN 2024bio	GOTO24it	60341.2564	60348.0188	6.748	3,600
SN 2024brg	2024brg	60345.2769	60350.8540	5.561	5,400
SN 2024bjk	2024bjk	60340.5962	60351.2326	10.63	2,273
SN 2024anm	2024anm	60327.6356	60351.2534	23.62	1,200
AT 2024bzq	GOTO24pj	60349.4191	60351.1370	1.702	5,400
SN 2024byg	2024byg	60348.5500	60351.1999	2.645	1,800
SN 2024cld	GOTO24ql	60353.2283	60353.2480	0.01971	2,400
			60354.1772	0.9382	3,600
GOTO24qj	GOTO24qj	60353.1556	60353.2032	0.04765	300
SN 2024cdt	2024cdt	60351.4380	60353.2242	1.776	2,472
SN 2024bzx	GOTO24pl	60349.5076	60353.1022	3.595	1,800
SN 2024bww	GOTO24oj	60347.9254	60353.9354	5.993	3,078
SN 2024ccf	2024ccf	60340.2940	60353.0186	12.71	1,961
SN 2024cew	2024cew	60351.2275	60354.2158	2.988	2,400
SN 2024cmh	2024cmh	60351.3710	60354.1353	2.764	1,800
AT 2024cmn	2024cmn	60353.2432	60354.1122	0.8582	2,446

[1]*Department of Physics, University of Warwick, Gibbet Hill Road, Coventry CV4 7AL, UK*
[2]*Centre for Exoplanets and Habitability, University of Warwick, Gibbet Hill Road, Coventry CV4 7AL, UK*
[3]*Astrophysics Research Cluster, School of Mathematical and Physical Sciences, University of Sheffield, Sheffield S3 7RH, UK*
[4]*Research Software Engineering, University of Sheffield, Sheffield, S1 4DP, UK*
[5]*Department of Physics & Astronomy, University of Turku, Vesilinnantie 5, Turku, FI-20014, Finland*
[6]*School of Physics and Astronomy, University of Birmingham, Birmingham B15 2TT, UK*
[7]*School of Physics & Astronomy, Monash University, Clayton VIC 3800, Australia*

Downloaded from academic.oup.com/mnras/article/552/3/stag1848/8836714 by guest on 21 October 2026

[8]*School of Physics & Astronomy, University of Leicester, University Road, Leicester LE1 7RH, UK*
[9]*Institute of Astronomy and Kavli Institute for Cosmology, University of Cambridge, Cambridge CB3 0HA, UK*
[10]*School of Physics, University College Cork, Cork, T12 K8AF, Ireland*
[11]*Department of Physical Sciences, The Open University, Walton Hall, Milton Keynes MK7 6AA, UK*
[12]*Department of Astrophysics/IMAPP, Radboud University, Postbus 9010, 6500 GL, Nijmegen*
[13]*Jodrell Bank Centre for Astrophysics, Department of Physics and Astronomy, The University of Manchester, Manchester M13 9PL, UK*
[14]*Instituto de Astrofisica de Canarias, E-38205 La Laguna, Tenerife, Spain*
[15]*Departamento de Astrofisica, Univ. de La Laguna, E-38206 La Laguna, Tenerife, Spain*
[16]*School of Sciences, European University Cyprus, Diogenes Street, Engomi, 1516 Nicosia, Cyprus*
[17]*National Astronomical Research Institute of Thailand, 260 Moo 4, T. Donkaew, A. Maerim, Chiangmai, 50180Thailand*
[18]*Armagh Observatory & Planetarium, College Hill, Armagh, BT61 9DG*
[19]*Institute of Cosmology and Gravitation, University of Portsmouth, Portsmouth, PO1 3FX, UK*
[20]*Centre for Astrophysics Research, University of Hertfordshire, Hatfield, AL10 9AB, UK*
[21]*The Institute for Globally Distributed Open Research and Education (IGDORE), Box 1074, Kristinehöjdsgatan 9A, Gothenburg, SE-412 82, Sweden*

This paper has been typeset from a TEX/LATEX file prepared by the author.

Downloaded from academic.oup.com/mnras/article/552/3/stag1848/8836714 by guest on 21 October 2026

© The Author(s) 2026.
Published by Oxford University Press on behalf of Royal Astronomical Society. This is an Open Access article distributed under the terms of the Creative Commons Attribution License (https://creativecommons.org/licenses/by/4.0/), which permits unrestricted reuse, distribution, and reproduction in any medium, provided the original work is properly cited.